AFIA: Aid For Investigating Accidents

A Major Qualifying Project Report

submitted to the Faculty of

WORCESTER POLYTECHNIC INSTITUTE

in partial fulfilment of the requirements for the

Degree of Bachelor of Science

by

Emilie Catherine Finken, RBE/ME

Zahava Preil, ME

Megan Throlson, RBE/ME

Date: May 6, 2021

Project Advisors:
Professor Kenneth Stafford, WPI
Bradley Miller, WPI

Abstract

In Ghana and other sub-Saharan countries access to robotics is extremely limited by the lack of materials and the cost of imports. The AFIA team developed a robot made mostly out of materials readily available in Ghana in the hopes that future designs like this can help make robotics more accessible. The robot is a multipurpose robotic platform designed to travel on poorly maintained dirt roads that are common in remote areas around the world and allows for the addition of sensors to fulfill the needs of the user. The goal of this project was to create an affordable, sustainable, multipurpose robotic mobile base to expand the availability of robotic technology.

Acknowledgements

The AFIA team would like to thank Professor Ken Stafford and Brad Miller for their advice, support, and troubleshooting help during this project. Thanks also to James Loiselle, Ian Anderson, and Elena Bachman for all of their help with the CNC lathes. Thanks to Professor Pradeep Radhakrishnan for his assistance with bond graph modeling, Squad for use of their woodshop, and the Academic City Students for their experience with engineering in Ghana. Thanks to the Robotics Resource Center for the use of their Robot cart and stapler in addition to use of the Higgins Machine Shop. Thanks to Alex Shiffman for helping us get started in Eagle. Thanks to Audrey McMahon for providing renderings of our CAD drawing. Thanks for Professor Nicholas Bertozzi, Olivia Caton, Audrey McMahon and Alex Shiffman for coming to our Preliminary Design Review and giving us feedback. Finally, thank you to everyone in the WPI robotics and mechanical engineering communities.

Table of Contents

List of Figures

List of Tables

Nomenclature Table

Acronym	**Meaning**
AFIA	Aid For Investigating Accidents
ANSYS	Analysis System
CAD	Computer Aided Design
COTS	Commercial Off The Shelf
FEA	Finite Element Analysis
GPS	Global Positioning System
IP	Ingress Protection
IRI	International Roughness Index
LiDAR	Light Detection And Ranging
MATLAB	Matrix Laboratory
MQP	Major Qualifying Project
NASA	National Aeronautics and Space Administration
OSHA	Occupational Safety and Health Administration
PSI	Pounds per Square Inch
PVC	Polyvinyl Chloride
SAE	Society of Automotive Engineering
SUV	Sport Utility Vehicle

WALRUS	Water And Lands Remote Unmanned Search
WPI	Worcester Polytechnic Institute

Table of Authorship

Section	**Author**
Abstract	Emilie Finken, Zahava Preil, Megan Throlson
Acknowledgements	Emilie Finken, Megan Throlson
1 Introduction	Emilie Finken, Zahava Preil, Megan Throlson
2. Background	Emilie Finken, Zahava Preil, Megan Throlson
2.1 Zipline	Zahava Preil
2.2 PlayPump	Zahava Preil
2.3 Ares	Megan Throlson
2.4 WALRUS	Megan Throlson
2.5 ORYX	Emilie Finken
2.6 Kinisi	Megan Throlson
2.7 Ingress Protection Standards	Emilie Finken
2.8 International Roughness Index	Megan Throlson
2.9 Social Implications	Zahava Preil

2.10 Goals	Emilie Finken, Zahava Preil, Megan Throlson
2.10.1 Size	Zahava Preil
2.10.2 Minimum Travel Speed	Emilie Finken
2.10.3 Thermodynamics and IP	Emilie Finken
2.10.4 Tele-op and Autonomous	Emilie Finken
2.10.5 Terrain Capabilities	Megan Throlson
2.10.6: Longevity	Megan Throlson
3 Design and Realization	Emilie Finken, Zahava Preil, Megan Throlson
3.1 Understanding Roads	Megan Throlson
3.2 Drivetrain Selection	Emilie Finken, Zahava Preil, Megan Throlson
3.3 Rocker Design	Megan Throlson
3.4 Rocker Prototyping	Emilie Finken
3.5 Rocker Construction	Zahava Preil, Megan Throlson
3.5.1 PVC	Megan Throlson
3.5.2 Brackets and Holders	Zahava Preil
3.5.3 Differencing Components	Zahava Preil
3.6 Stress Analysis	Emilie Finken
3.7 Wheels	Emilie Finken, Zahava Preil

3.8 Motor Selection and Gear Ratio Calculation	Emilie Finken
3.9 Batteries	Emilie Finken
3.10 Box Design	Megan Throlson
3.11 Box Construction	Zahava Preil
3.12 Cooling System	Megan Throlson
3.13 Board Selection	Emilie Finken
3.14 Sensor Selection	Emilie Finken
3.15 Teleoperation Control	Emilie Finken
3.16 Board Layout	Megan Throlson
3.17 Code Design	Emilie Finken
3.18 Code Implementation	Emilie Finken
4 Results	Emilie Finken, Zahava Preil, Megan Throlson
4.1 Size Goal	Zahava Preil
4.2 Travel Speed	Emilie Finken
4.3 Thermodynamic Analysis	Megan Throlson
4.4 IP Goal	Emilie Finken
4.5 Code Capabilities	Emilie Finken
4.6 Terrain Capabilities	Megan Throlson
4.7 Battery Goal	Emilie Finken

4.8 Growth Potential	Zahava Preil
4.9 Material Considerations	Megan Throlson
4.10 Overall Design and Construction	Zahava Preil
5 Conclusions	Emilie Finken, Zahava Preil, Megan Throlson
5.1 Recommended Improvements	Emilie Finken, Zahava Preil, Megan Throlson
5.1.1 Handling Loads	Zahava Preil, Megan Throlson
5.1.2 3D Printing	Emilie Finken
5.1.3 Parts Acquisition	Zahava Preil
5.1.4 Design for Construction	Zahava Preil
5.1.5 PCB Design	Megan Throlson
5.1.6 Testing Earlier	Emilie Finken
5.2 Areas of Strength	Emilie Finken, Zahava Preil, Megan Throlson
5.2.1 Teamwork	Zahava Preil
5.2.2 Parametric CAD	Megan Throlson
5.3 COVID-19 Considerations	Emilie Finken
5.4 Future Potential	Megan Throlson
5.5 Overall Conclusions	Zahava Preil

References	Emilie Finken, Zahava Preil, Megan Throlson
Appendix A: Pictures of Ghanaian Roads	Megan Throlson
Appendix B: Key Project Dates	Emilie Finken
Appendix C: Budget Estimate	Megan Throlson
Appendix D: Full PVC Stress Calculation	Emilie Finken
Appendix E: Full Motor and Gear Ratio Calculation	Emilie Finken
Appendix F: Motor Curve Data	Emilie Finken
Appendix G: Full Battery Calculation	Emilie Finken
Appendix H: GrabCAD Link	Megan Throlson

All sections of the paper were edited by all team members. There was also significant collaboration on all sections of the paper.

1. Introduction

In Ghana and other sub-Saharan countries, the combination of remote, poorly traversed dirt roads, unreliable technologies such as lack of cell phone service coverage, and little to no enforcement of safety standards make traveling along these roads extremely dangerous. When accidents occur, the people involved must rely on passersby for assistance. While most people in Ghana will stop and go out of their way to help, waiting for the unreliable possibility of someone coming along wastes valuable time, especially in cases of head wounds or severe bleeding. One such case was in January of 2020 when a bus full of WPI students, traveling back to their project housing from a weekend trip, encountered a motorcycle accident involving a group of people, including a young girl. It was apparent that the girl had suffered a head wound, and that she and her companions had been there at the roadside for a while. While they were fortunate to encounter the bus, which was able to take them to a local health center, valuable time was lost in the wait. Our hope with this project was to begin closing the time gap between when the accidents happen and when a rescue team arrives via automation. This would be accomplished by use of robots that can traverse the difficult terrain, are sustainably made with readily available resources, and can be easily maintained by locals. While this project was designed to be a multi-purpose robotics platform, keeping with our motivation, we used this mission scenario of surveying roads in remote areas of Ghana for accidents to guide our design.

To make our project effective in helping these communities, we needed to keep sustainability in mind throughout our design process. In our context, this meant achieving two of our primary goals, longevity and availability, in our final robot design. Resources and materials readily available in a WPI robotics lab were often unattainable or inaccessibly expensive to ship to Ghana. While we were designing a system that was as durable as possible, we understood that the robot would be operating under strenuous conditions and would likely break down over time. To ensure that the robot could remain in service, it was important to consider the ability to make repairs in the country. It was not enough to pick the strongest, longest-lasting, most environmentally conscious materials. Material selection also had to keep in mind what is accessible in Ghana; the “best” material as defined by our engineering textbooks was not the best choice if the robot would not be buildable and could not be maintained.

We designed and built a robotic base that could traverse the rough terrain of unmaintained roads with little human contact or intervention. It needed to be durable and stable, able to navigate over or around nonuniform obstacles such as fallen branches, ditches, gravel beds, and miscellaneous detritus, as well as be shielded from the elements.

In keeping with our mission scenario and our growth platform ideology, we used a standard bolting pattern panel to allow for additional sensors and mechanisms. We designed an electrical system with the ability to add new sensors. As with the base, this board was designed to utilize components that are low cost and sustainable whenever possible. Given the lack of electrical components widely available in Ghana, it is likely this would have to be largely imported.

We researched projects with similar design criteria or operating under similar conditions. The information gained from this research influenced the measurable goals of the AFIA (Aid For Investigating Accidents) project.

2. Background

2.1 Zipline

Zipline is a California-based company founded in 2014 that manufactures drones, with the goal of utilizing them to ultimately make medical supplies instantly accessible anywhere in the world. In 2016 they launched in Rwanda and within three years, Zipline drones were responsible for over 13,000 deliveries of blood products [1], before expanding into Ghana. Healthcare providers send in a text message to a supply center, which can have a drone packaged, launched, and delivered in an average of 30 minutes to anywhere in that supply centers' radii [2], whereas without Zipline the poor roads and medical infrastructure, refills of medications could instead take months, and emergency blood products and antivenoms would be unable to reach life or death situations. For well supplied hospitals and clinics in populous areas, the idea of spending medical funds on miniature airplanes when they can order and store the appropriate supplies on hand reliably seems frivolous at best [3]. But consider the remote clinics, which take hours to reach and often run out of medications before they can treat everyone present. Once patients have committed that time only to be turned away untreated, they are increasingly reluctant to return and try again, losing access to lifesaving services. Instead, those medications can be refilled via Zipline.

2.2 PlayPump

The Roundabout PlayPump Water System was invented in South Africa in 1989 [4] and praised for its ingenuity in addressing the severe issues arising from lack of access to potable water in developing countries. The PlayPump replaces a traditional manual water pump with a children's merry go round, designed to be able to supply communities with water from only the work of kids having fun. The system gained attention after Nelson Mandela attended a school opening in 1999 where PlayPump was in use and was rolled out to communities across the country. By 2010, however, the system had come under international criticism as being difficult to maintain and expensive to repair, a poor solution to areas where the issue was not simply water shortage due to pumping difficulties, and most damning, "that kids would have to "play" for 27 hours a day to meet the target of delivering water to 2,500 people per pump" [5].

2.3 Ares

Another robot that caught our attention was Ares, a humanitarian demining robot created by a joint partnership between the Portuguese SME IntRoSys, the New University of Lisbon, and LabMAg research centre of the University of Lisbon. This robot was designed to go into fields with land minds, find these land mines and denote them. This is important work because it is very dangerous for humans, and because of this a variety of different robots have been designed to do this work, but many of them are hard to operate and very expensive. Because of this the robots are often not used. The Ares team attempts to address this problem by designing a simple demining robot that is also low cost, so that it can be easily used by the communities affected by these mines. To pass through uneven terrain the robot uses four different locomotion modes (Double Akerman Mode, Turning Point Mode, Omnidirectional Mode, and Lateral Mode), while utilizing a flexible chassis. All four wheels are independently controlled [6]. Ares shows that it is possible to make an effective all-terrain robot utilizing mostly readily available materials.

Figure 1: Ares Robot [7]

2.4 WALRUS

In addition to researching outside projects, we also looked at several MQPs. One of the MQPs we investigated was WALRUS (Water And Land Remote Unmanned Search) as seen in Figure 2. WALRUS was completed in 2015 and was designed to handle a variety of rescue missions. To accomplish these missions, WALRUS is capable of multiple skills including climbing up stairs, swimming, and navigating through hallways. This was accomplished by utilizing four flippers and a tank drive system with tread. The WALRUS robot is designed to be a growth platform, with interchangeable payloads, on a standard hole pattern base.

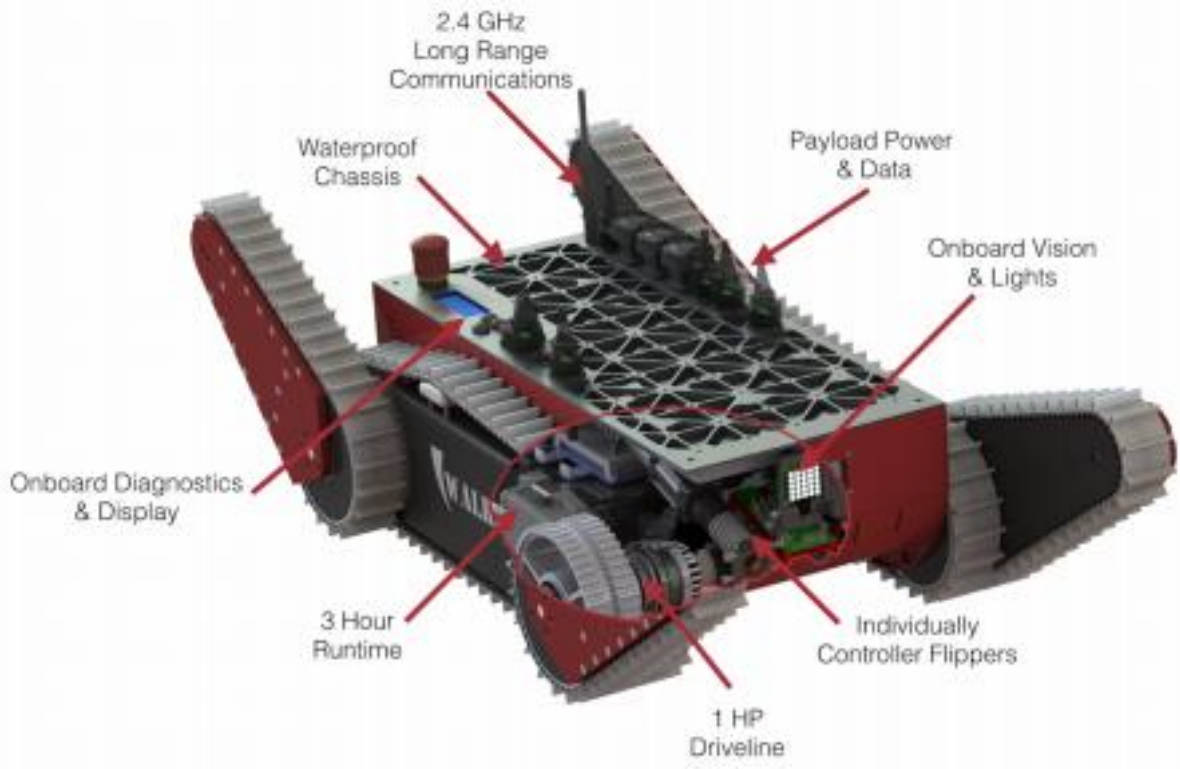

Figure 2: WALRUS

WALRUS was designed to be versatile and could go on a variety of mission scenarios everywhere from navigating in an apartment complex to swimming in hurricane waters. One such scenario the WALRUS team considered was the robot being used to deliver medical supplies to remote African villages during a pandemic. This seemed in line with the AFIA project; however, WALRUS possessed a variety of additional, unnecessary features for our mission scenario, which became a detriment when cost was a hindrance to shipping robots to Sub-Saharan Africa [8]. For our project, it made more sense to design a robot for Ghana that

focused on being low-cost and could be built in the country as much as possible, rather than building in extra capabilities.

2.5 ORYX

ORYX 2.0 was a WPI Robotics MQP from 2011. The robot was designed to be a planetary exploration rover for the NASA (National Aeronautics and Space Administration) RASC-AL Robo-Ops challenge. ORYX was built to meet specific competition requirements based on previous NASA rovers challenged to drive over rough terrain. Additionally, the rover needed to be capable of operating on Earth in analogous testing locations. Along with working to meet the competition requirements, the MQP team set additional goals for themselves to make the robot more accessible for future missions; it was designed to be easily customized and low cost in comparison to other planetary exploration vehicles [9].

The Robo-Ops rules required all rovers to be able to overcome obstacles of 10 cm and inclines of 19 degrees; the ORYX design accounted for 15 cm obstacles and 30-degree inclines. This goal was met using a derivative of the rocker-bogie suspension system [9].

Figure 3: ORYX Rover

The rocker bogie system has been used on NASA rovers for over 20 years with incredible success, allowing rovers to drive over steep slopes and obstacles greater than their wheel diameter. A full six-wheel rocker-bogie suspension was deemed unnecessarily complicated for the Robo-Ops challenge. The suspension system required a complicated 5 bar linkage in order to provide more capabilities than were necessary to meet the challenge goals. The simplified four-wheel rocker linkage suspension used on the Carnegie Mellon Red-Rover had the necessary incline and obstacle drive capabilities to accomplish the goals. The simplified rocker suspension system improved stability, obstacle interaction, and weight distribution when compared to a fixed chassis. This suspension system was the middle ground between a full NASA rover and more standard fixed chassis robot suspension systems. Coupled with carefully selected wheel size, a four-wheel rocker suspension system allowed the rover to meet the challenge goals while limiting unnecessary design complications [9].

The ORYX rover was sealed to protect the electronics and motors from dust and water. The Robo-Ops competition only required that rovers be capable of operating in light rain. However, the MQP team wanted the rover to be capable of full testing on Earth, which required the electronics box to be protected. Completely contained electronics boxes are common on NASA rovers, since dust is capable of damaging electronics. The regolith found on the moon is especially abrasive. The only way to prevent the ingress of harmful dust is to seal the electronics box, which also prevents water from entering. As the ORYX rover was designed to be capable of extraterrestrial exploration, rather than just to complete the Robo-Ops challenge, sealed electronics were necessary to meet the team's design goals. The distinction between an earth exploration rover and an extraterrestrial rover is most clearly made in the temperature regulation devices included onboard. By sealing the electronics, ORYX had to develop a system to prevent incurring damage from overheating during analog testing. In contrast, for true extraterrestrial rovers, electronics must be heated against the cold void of space. ORYX's electronics served as a thermal generator, and with the sealed enclosure preventing ventilation, an alternate cooling method was required. The MQP team used an off the shelf water-based cooling system to keep the overall robot cost down. This system was not acceptable for space exploration but was necessary for the analog testing and Robo-Ops competition [9].

The final important aspect of ORYX was the customizable design. ORYX was designed to be used for a variety of terrestrial and extraterrestrial explorations. This was accomplished through standard mechanical and electrical interfaces. The ORYX rover utilized USB connections to provide standard power and modular mechanical payload interfaces. This allowed for payloads to be easily designed and integrated into ORYX without requiring the addition of specialized mechanical or electrical connections [9].

The ORYX rover MQP included a variety of well-designed systems ranging from suspension for driving on rough terrain to electronic interfaces for modularity that are applicable to the AFIA project. By researching the goals and designs of this project we gained a better understanding of how to approach the main goals of our project.

2.6 Kinisi

We also looked at Kinisi, an MQP completed in 2019. The Kinisi team worked to convert an SAE (Society of Automotive Engineering) Baha vehicle to be fully autonomous. While self-driving capabilities were out of the scope of our project, planning for them increased the potential uses of AFIA. It was useful to see how the Kinisi team achieved self-driving capabilities, so we could consider how to leave room for similar sensors and equipment on the AFIA robot. We paid special attention to the sensors Kinisi used to detect and map the environment around them, as obstacle detection was within the scope of AFIA. To do this the Kinisi team used 5 sensors: Intel® RealSense™ Depth Camera, a SICK 3D LiDAR, a GPS module, and two consumer-grade motion sensors. To ensure that AFIA had room to have these obstacle avoidance sensors in the future we needed to leave at least 5 ports for these or similar sensors to be added [10].

2.7 Ingress Protection Standards

Dust, water, and heat are capable of damaging electronic components. Dust and water can cause short circuits, while heat decreases the operational life of components. The IP (Ingress Protection) code rates consumer devices on a dustproof scale from one to six, and a waterproof scale from one to nine. These scales go from no protection against dust and water to completely protected. The average consumer product is rated as IP5X, meaning the product is protected

against dust but not completely dustproof. The X indicates that there is not a number specified for waterproofing [11]. Below in Table 1, IP code ratings are provided with their specific definition.

Number	Dust Protection	Water Protection
0	No Protection	No Protection
1	Protected against any solid objects greater than 50 mm in size	Protected against water drops
2	Protected against solid objects greater than 12.5 mm in size	Protected against water drops at a 15-degree angle
3	Protected against solid objects greater than 2.5 mm in size	Protected against water spray at a 60-degree angle
4	Protected against solid objects greater than 1 mm in size	Protected against water splashing from any angle
5	Protected against access to hazardous parts and dust	Protected against water jets from any angle
6	Protected against access to hazardous parts, dust-tight	Protected against powerful water jets and heavy seas
7	-	Waterproof for 30 minutes at 1 m depth
8	-	Protected against the effects of temporary submersion
9	-	Protected against high pressures associated with steam cleaning

Table 1: IP Code Definitions

Projects like WALRUS and ORYX were designed to be dust and water resistant for their missions. These sealed systems required specific attention be paid to energy dissipation. Electric components generate heat during operation, and sealed enclosures complicate energy removal. Conduction through enclosure walls is inefficient unless there is a drastic temperature difference between the interior and the exterior ambient temperatures [12]. The amount of thermal energy that needs to be dissipated from a system is based on the safe operating temperatures of the batteries, sensors, controllers, and motors in the system. The method of dissipation is determined by the amount of energy and the mission parameters. Two common methods for regulating temperature in enclosed spaces are fans and liquid-based cooling systems.

2.8 International Roughness Index

To design a robot that can transverse a variety of different types of roads, we must first understand how roads are classified. The most common way to classify roads is by the quality of the driving surface using the IRI (International Roughness Index). The IRI is calculated using the block diagram of the quarter car, as seen below (Figure 4) [13].

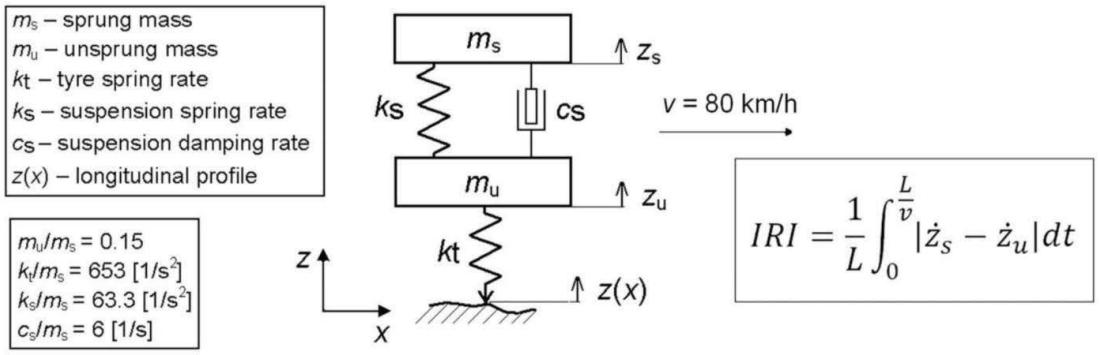

Figure 1. Quarter-car model for IRI estimation.

Figure 4: Quarter Car Model for Calculating IRI [13]

An accelerometer is placed on both the sprung and unsprung mass. Using the measurement from the accelerometer, the velocity in the z-direction is derived. This can then be added into the equation from Figure 4. It is important to note while this is traditionally how the IRI is calculated, there are other methods used mostly in developed countries. In the United States it is common to shine a light on the road, and then measure the shape the light makes on the road.

This is less expensive than measuring with the quarter car model. Depending on the method variances can occur in the IRI, but we do not anticipate that impacting this project [13]. Because the IRI is calculated using the quarter car model and is related to the difference in velocity of the sprung and unsprung mass, it is not directly related to our project and must be converted to a more applicable measurement. In this case, we are interested in what is the input of the road in our system given a certain IRI. To calculate, we derived an equation in terms of X' = AX +BU, where A, X, and B are given matrices from the paper, U in the input from the road we are solving for and X' in based on the given IRI. Below is the equation we are using to convert the IRI to a usable value. In this equation, $K_1 = 653$; $K_2 = 63.3$; C= 6, $\mu = 0.15$ and L = 250. Since the IRI is an average of multiple spots on a road, IRI designates the given spot that we are currently examining [13].

$$\begin{bmatrix} L*IRI[i] \\ IRI[i]-IRI[i-1] \\ L*IRI[i] \\ IRI[i]-IRI[i-1] \end{bmatrix} + \begin{bmatrix} 0 & 0 & 1 & 0 \\ 0 & 0 & 0 & 1 \\ -1 & 0 & 0 & 0 \\ 0 & -1 & 0 & 0 \end{bmatrix} \begin{bmatrix} Z_s' \\ \dot{Z_s}' \\ Z_u' \\ \dot{Z_s}' \end{bmatrix} = \begin{bmatrix} 0 & 1 & 0 & 0 \\ -K_2 & -C & K_2 & C \\ 0 & 0 & 0 & 1 \\ \frac{k_1}{\mu} & \frac{C}{\mu} & \frac{K_2-K_1}{\mu} & \frac{-C}{\mu} \end{bmatrix} \begin{bmatrix} Z_s \\ \dot{Z_s} \\ Z_u \\ \dot{Z_s}' \end{bmatrix} + \begin{bmatrix} 0 \\ 0 \\ 0 \\ \frac{K_2}{\mu} \end{bmatrix} [u] \quad (1)$$

2.9 Social Implications

Something expensive to build and difficult to maintain will only have the lifespan of its initial parts. Our robot's first mission would be its last if the robot could not be repaired when the need arose. A notable example of a successful project is Zipline's medical supply drones, which have been running in Ghana for a little over a year and exceeding their goals for lifesaving deliveries of blood, antivenom, vaccines, and other medical supplies previously impossible to get around the country in a timely manner. However, since its introduction in the country it has been harshly criticized, seen as a frivolous and impractical project taking focus away from "real" problems. PlayPump had the opposite experience; its initial hype was so celebratory that the project was rolled out on a large scale too quickly to realize its myriad underlying faults, causing any number of problems in communities it had been designed to help. For our project, we aimed to not only design and build something that would work, but would be understood and accepted by, as well as genuinely useful to, the communities it serves. This goal was reflected in our design in several aspects including visually, to design something people would not fear. There is very little public

familiarity with robots in Ghana, making a friendly, unintimidating appearance all the more important. In addition, the mission scenario parameters were kept in mind for the mechanical components; as much as possible, our robot is buildable in the country and repairable locally, keeping the project community-oriented, rather than just another wasteful high-tech project dropped in by outsiders who did not understand the real issues present and how to address them.

2.10 Goals

Goal	Primary	Secondary
Size	Upper Bound: 4ft by 2.5 ft by 2.5 ft. (Disassembled) Lower Bound: 2 ft by 1 ft by 2 ft	N/A
Weight	Upper Bound: 100lb per section	N/A
Minimum Travel Speed on Flat Terrain	4 miles per hour	5 miles per hour
IP code	IP 54	IP65
Maximum Ambient Operating Temperature	90 F	100 F
Terrain Capabilities	IRI 11	IRI 16
Battery Life	2 hours	4 hours
Additional Sensor Capabilities	10 Sensors	N/A
Payload Capacities	20 pounds	50 pounds

Table 2: AFIA Goals

2.10.1 Size

Since AFIA was designed for traveling on roads, we needed to decrease the chance that drivers would hit the robot. To do this we needed the robot to be large enough that a driver could easily see it, as well as large enough that a driver would be incentivized to navigate around the robot and not hit it. To do this the robot was designed to be no shorter than two feet, with a base no smaller than two feet by one foot.

At the same time, we wanted to make the robot easy to transport, in case it broke down and could not drive itself. From looking at our own mid-size cars we determined that a reasonable size for

the robot in travel configuration to be 2.5 feet by 2.5 feet. If disassembly were to be required, the disassembly and reassembly process would be doable by two people, with common hand tools, and take no more than 10 minutes from the start time to when the robot is put in the car.

In order to allow for the robot to be able to be lifted and put into a car by no more than two people, when the robot is disassembled into its travel configuration, no section of the robot may weigh more than 100 pounds. This comes from the OSHA standard that one person may not lift more than 50 pounds.

Due to the range of possible sizes for AFIA, a variety of factors were taken into account. An important consideration was the relationship between size and the difficulty of cooling the robot. Because area increases exponentially with the increases in robot size, even small changes could add complexity in the cooling system design. On the other hand, a bigger robot would increase the space for drivetrain elements and increase the size difference between obstacles faced by the robot and its drivetrain, meaning more clearance.

2.10.2 Minimum Travel Speed

The velocity at which the robot must be able to travel was based on the desired battery life and the distance between regional capitals that are located around Accra, Ghana. These cities are typically located between 15 and 20 miles apart. Using the shorter distance, 15 miles, and the second-tier battery life goal of four hours, the robot was required to travel at a speed of four miles per hour. This represents the minimum speed of travel on flat ground; lower speeds may be necessary to safely traverse obstacles. The secondary travel speed goal is five miles per hour to accommodate the longer distance between regional capitals. At just above walking speed, this did not place the electronics in danger of excessive jostling.

2.10.3 Thermodynamic and IP

The AFIA mission scenario expands on one potential use of this modular robotic platform. Specifically, it calls for the robot to operate in Ghana. This supplies specific ingress protection

and temperature control guidelines similar to the ORYX and WALRUS mission scenarios. The Ghanaian climate and landscape guided us in the creation of the temperature control and ingress protection goals, outlined in Table 2.

The ingress protection goals are the minimum IP code ratings acceptable for the Ghanaian climate. Ghana experiences an annual rainy season in the north lasting from April to October, and two rainy seasons in the south, April to June and September to November [14]. During this time minor flooding is common, and the robot would likely become wet from not just the rain, but also from driving through standing water. Since the AFIA mission scenario requires the platform to operate in the elements year-round, waterproofing is necessary. The primary goal was IPX4, meaning the robot had to be protected from water splashing at any angle. This primary goal set a standard of protection against both rainfall and splashing. The secondary goal of IPX5 required that the robot be able to withstand water jets from any angle. This was a secondary goal because it was not necessary for basic operation and served as an increasingly conservative level of water protection. IPX4 is the minimum amount of water protection that will be sufficient to meet the mission scenario; extra water protection was preferred, but not necessary.

The second part of the ingress protection goals related to dust protection. The AFIA platform had to be capable of operating on dirt roads. No matter where in the world the dirt road is located, dust interfering with electronic components is a potential hazard. The amount of dust entering the system had to be limited to ensure the electronic components are not shorted. This was achieved with the standard consumer level of dust protection, IP5X. Dust will be kicked up while the robot operates but the dust protection common to other electronic systems will ensure the robot remains capable of operating**.** As with water protection, the minimum goal is IP5X, but if the system is capable of being entirely dust tight, IP6X, that would be preferred.

The specific mode of temperature control was based on what systems are capable of efficiently dissipating heat without allowing for the ingress of water or dust at levels above the previously stated goals. It must meet the baseline temperature regulation goals as based upon common temperatures in Ghana specified in the mission scenario. The primary goal is for the robot to be able to operate in 90-degree Fahrenheit temperatures for the duration of testing. The secondary

goal is for the robot to be able to operate at 100 degrees Fahrenheit for the duration of testing. The tertiary goal is for the robot to be able to operate in 100-degree Fahrenheit weather for 13 hours. All of the tiers for temperature control are based on the hottest Ghanaian temperatures in different regions. The north of Ghana has the highest temperatures, where it can be upwards of 100 degrees, but in the capital of Accra, the temperatures peak around 90 degrees [15]. The tier three timing goal is based on the fact that the maximum temperatures occur during daylight hours, with the sun contributing most of the heat. The longest day is the summer solstice which, in Ghana, provides thirteen hours of daylight. If the robot was capable of temperature regulation for thirteen hours, the system would be robust enough to withstand common Ghanaian conditions. This timing was only applied to the tier three stretch goal as it was above what is necessary for the successful completion of the mission scenario, and unreasonably challenging to prove during a New England winter.

2.10.4 Teleoperation and Augmented Autonomy

AFIA needs to be applicable to many situations, making teleoperation and augmented autonomy vital. The goal for teleoperation and augmented autonomy is that the code must be robust enough to complete the drive system testing. Teleoperation must allow for line-of-sight control of the platform, and the augmented autonomy programming must be capable of driving the robot through a known obstacle detection course. This course will be designed with obstacles of increasing sizes. The robot will be expected to either drive over or stop before an obstacle based on if it is safe to continue. The key aspect of augmented autonomy for this project is that it must detect obstacles and determine if the robot is capable of overcoming them. The code must stop the robot if driving over an obstacle will cause the robot to tip or get stuck. This code will lay the groundwork for future uses by providing basic augmented autonomy and short-range teleoperation.

2.10.5 Terrain Capabilities

As discussed in Section 2.8, IRI is the most common way to classify the quality of a road. The IRI is a calculated number, but we cannot gather data related to the conditions of our mission scenario. An attempt has been made to reach out to the Ghanaian Ministry of Highways and

Roads though we never received a response. We instead did our best to estimate the IRI based on images of these Ghanaian roads (Appendix A). To make the most educated guess possible we have used Figure 5 from Pavement Interactive [16].

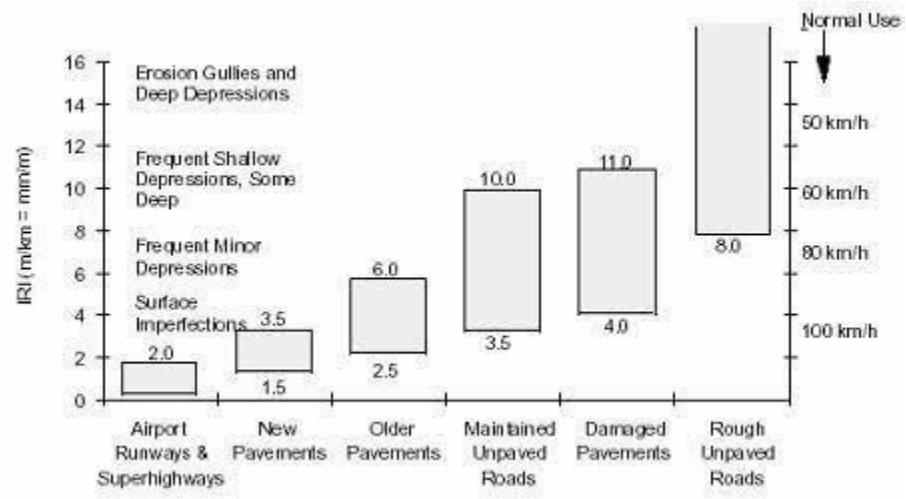

Figure 5: Ranges for Given Road Types [16]

Given this information, we are setting a primary goal of being able to drive on roads of an IRI 11mm/m or lower. This should allow us to drive on older pavement, maintained unpaved roads, damaged pavements, some rough unpaved roads, and any roads in better conditions. This encapsulates the majority of Ghanaian roadways that will be patrolled in the mission scenario. As a secondary goal, we would like to drive on roads of and IRI 16 mm/m or lower. This should give us the added benefit of being able to drive through Erosion Gullies and deeper depressions. We are defining the ability to drive on roads of IRI Xmm/m as being able to drive over obstacles up to the 95th percentile in size where we assume a Gaussian distribution around the IRI value, with a variance of the given IRI divided by 10.

2.10.6 Longevity

To ensure the usefulness of AFIA, we wanted to think about how the robot could be used and how to design the robot in a way that it will be long-lasting. Unlike the previously stated requirements, this idea is much more abstract, and cannot be easily defined by measurable engineering standards. We directed our research to come up with what we felt were reasonable,

yet somewhat arbitrary goals. Longevity is broken down into subgoals, as follows: The operation time of the robot, the ability of the robot to be used for numerous purposes, and the reparability of the robot.

Energy is crucial to the success and longevity of the AFIA project. As a mobile robotics platform, it will be powered by rechargeable batteries. Battery selection must be based on the mission scenario, testing time, and the lifespan of the battery. Battery life decreases as operating temperature increases, the battery selected must be capable of safely operating within the temperature range specified by the temperature control goal. The battery weight-to-voltage ratio must also be researched. As AFIA is intended to be a multi-purpose modular platform, the trade-off between batteries and payload capacity must be considered. The best option is to design the platform to accept additional batteries over the selected testing amount. This way, should a future use require longer operational time, the payload capacity can be decreased to accommodate additional batteries**.** The AFIA batteries must last for a minimum of 2 hours to provide for adequate testing and meet the travel speed and payload capacity goals. The weight and cost of batteries and the energy necessary for a 150-pound platform to travel at 4 miles per hour makes operating for a long period expensive and challenging. In order to keep the overall robot cost down the battery life has been set to facilitate testing rather than cross country travel. For uses that require longer operational life additional batteries can be added. The robot must be capable of carrying extra batteries to increase the operational life depending on the desired use.

Once a target weight and velocity were ascertained preliminary motor sizing began. The first step was to determine the power necessary to drive the robot. In order to make the estimation as accurate as possible the robot was assumed to be driving up a slope. The goals for weight and velocity were used as well as an estimated slope of 15 degrees. The overall power required to drive a 150-pound robot up a 15-degree incline at 4 miles per hour is 386 Watts. This is distributed among four drive motors resulting in roughly 96 Watts per motor as in shown in Equation 2.

$w := 150lbf \quad v := 5mph \quad i := 15deg$ Variables, w = Weight, v = Velocity, i = Incline

$P := w \cdot v \cdot \sin(i)$ Watts required to drive up incline

$P = 386.003\,W$

$P := 386W$

$\frac{P}{4} = 96.5\,W$ Watts per motor, currently 4 motors (2)

Our robot will be designed to be able to attach a variety of accessory payloads, up to ten interfaced sensors or 20lbs of gear. To accomplish this, we will be including standard payload interfaces such as USB ports and controlled power levels of varied voltages (5V, 12V, etc.). Additionally, we will include the capacity to easily attach non-electrically interfaced gear, such as a first aid kit. This customizability will make our system flexible enough to be applicable to any variety of mission scenarios.

One major design consideration for the project is to allow for as much of the building and repair of the robot as possible to be done in-country. This will help reduce the cost of the robot to make it more manageable for the developing country, as well as reduce turnaround for repairs. While measuring the actual time it takes to make repairs is not possible, we will do our best to design the system to be repaired quickly and easily.

Tier 1	Tier 2	Tier 3	Tier 4
Materials are easy to find in villages in addition to the cities	Materials can be found in cities but may not be found in villages	Materials are difficult and expensive to get and can only be found in cities.	Materials must be imported for this project and will be expensive to get
• PVC pipes (different sizes) • Rope/String • Hard Woods • Nails • Some bolt sizes (small selection) • 1 Cedi Chinese super glue and Epoxy • Colorful cotton cloth (but cities will have it cheaper and with more variety) • Cardboard • Plastic bottles • Clear plastic Tupperware • Laundry Buckets • Door Hinges • Manual Sewing Machine parts	• Screws of all sizes • Bolts of all sizes • Scrap Car parts • Springs • Variety of wheel types • Tread (using for the grinding mill) • Wire (some imports) • Metal cable (some imports)	• Metals like aluminum and steel • Scrap Motorcycle parts	• “hobby circuit boards” such as Arduino or ESP32 • Prebuilt all-terrain robots

Table 3: Material Tiered Systems

This list was constructed with the help from Academic City College University student, Gertrude Akunlibe.

For the electronics box repairs to be completed in the village, all materials would be from tier 1, or easily kept in villages and fixed with available tools. For the drivetrain to be fixed in cities, materials should be tier 1 or 2, but tier three is possible if there is strong reasoning and a plan to get the material if that section needs to be fixed.

Another consideration of repairability is the availability of tools to perform the actual repairs. In the villages, most of the tools are for woodworking and sewing. In the cities, there will be machine shops, as seen below in Figure 6.

Figure 6: Academic City Machine Shop

3. Design and Realization

3.1 Understanding Roads

One of the largest challenges we faced was to determine what type of obstacles the robot would need to be able to go over. This was especially difficult as we could not take measurements from the roads we wished to drive over. In the proposal, we explore the possibility of using the IRI of the roads, but after learning more about this topic and attempting to reverse engineer the IRI, we found this to be impractical for this project. The IRI utilizes an ideal car model and measures the difference in position for the sprung and unsprung mass. Because of this, the equation used to derive the IRI is a differential equation, and with no experimental data, fairly complicated to derive. To model the road, we instead chose to look at an obstacle with a max height of 6 inches above ground level, and a maximum ditch depth of 6 inches below ground level. To make a sample road we assumed a normal distribution around 0, and 99.9% of the road being under the max height. We assumed that anything exceeding our obstacle and ditch bounds will be

circumvented by the robot, so we treat anything over the max height or ditch depth as if it were the max height or ditch depth respectively.

3.2 Drivetrain Selection

In order to operate on the unmaintained roads in Ghana, we had to select a drivetrain that would be able to handle the rough terrain, be easily maintainable, and be realistic to make out of locally sourced, durable, sustainable materials. We evaluated each of our considered drivetrain systems based on their ability to handle rough terrain, agility for navigating obstacles, simplicity of the system to build and maintain, running speed, ease of repairability, system size, and system cost. We used a weighted decision matrix to evaluate our options. Size had a multiplying weight factor of 1, reflecting that it was a consideration to keep in mind in the selection process, but not a strong one, as meeting our goal of fitting AFIA into an SUV (Sports Utility Vehicle) trunk can be accomplished via partial disassembly into travel configuration. Agility had a weight of 2; while portability matters, it did not hold as high of a significance as the ability to navigate around obstacles in our mission-scenario environment. Speed and repairability each had a weight of 4. By valuing a drivetrain system that was easily repairable, we planned for the future of the system, so fixes to it would be possible locally and quickly with on-hand components. Speed, like agility, factors into the robot's ability to operate under mission scenario parameters; selection of a drivetrain with those capabilities enabled our robotic platform to be useful in real time. Simplicity had a weight of 5; like repairability, this was a component weighted to help select the superior drivetrain for our specific mission scenario of environments with limited access to robotics equipment and familiarity. As much as possible AFIA is to be built and maintained locally, so vital components like the drivetrain need to be as easily buildable as possible. Cost had a weight of 6; an expensive drivetrain, and robot overall, could accomplish our goals of handling rugged landscapes in hot weather without being damaged by dust or rain, but keeping cost in mind as we made this selection and the rest was paramount to realizing our goal of designing and building not just a functional robot, but a sustainably low-cost one. Finally, terrain capability had a weight of 7. If our drivetrain, and therefore our robot, cannot handle mission-scenario rough terrain, it cannot be used, making this category of highest importance.

	Terrain Capabilities	Agility	Simplicity	Speed	Repairability	Size	Cost	
Weighting	7	2	5	4	4	1	6	Total
Ackerman	4	8	5	7	5	8	7	167
Tread	8	5	4	5	2	7	2	133
Rocker Bogie (6 wheels)	9	9	5	7	7	6	5	198
Red-Rover Rocker	8	5	6	7	8	7	6	199

Table 4: Drivetrain Decision Matrix

For our drivetrain, we considered the options of an Ackerman system, tank tread, six-wheel rocker-bogie, and a Red-Rover style rocker. An Ackerman system utilizes a four-bar linkage to change the angle of the front wheels. By changing the angle of the front wheels, the direction of the robot is changed. This reduces the slip in the tires when rounding corners. It is commonly found in cars, and robots that need high agility.

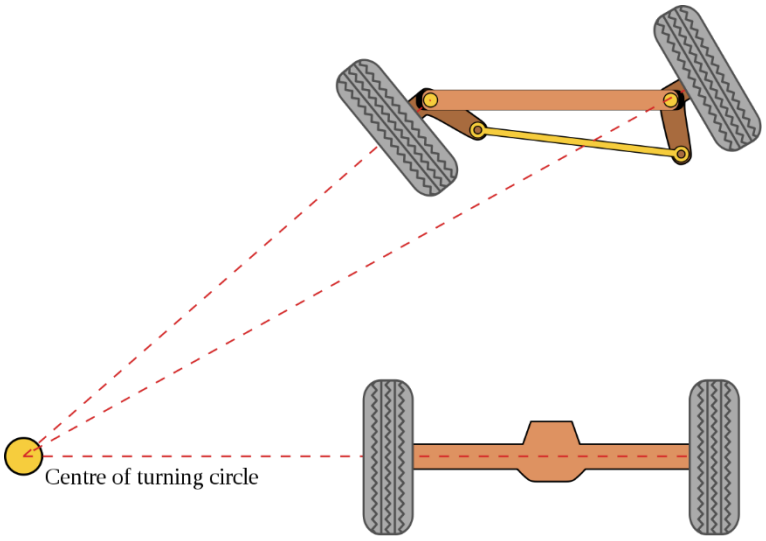

Figure 7: Ackerman Steering [17]

After investigating Optimal Driveline Robot Base MQP [18], we discovered that in order to drive each wheel independently we would need a complicated linkage system, resulting in more potential points of failure and more challenging maintenance. Given our goal regarding repairability additional design complications were undesirable. Most of the roads in Ghana are relatively straight or at least have very large curves, agility is not a primary concern, so the

additional complexities of the Ackerman steering do not provide the benefits that would be required to move forward with this idea.

Tank tread utilizes a continuous band of tread around two or more sprockets to evenly distribute a vehicle's weight. This even distribution over a large surface area allows tread to maintain better contact with the ground as opposed to wheel-based drivetrains, giving tank tread an advantage in avoiding becoming stuck on soft surfaces. This terrain capability is what made tread an attractive consideration for addressing our rough terrain goals. However, if any segment of the tread breaks, the full tread is immobilized, and it can sometimes become jammed or misaligned, or come off the wheels. In addition, tread must be correctly tensioned to the wheels using variable tensioners even as it traverses obstacles, which can be challenging to set. All of this introduces a level of complexity and cost to the maintenance at odds with our sustainability, simplicity, and repairability goals.

Figure 8: Tank Tread on Bulldozer [19]

The Rocker Bogie drivetrain was originally designed by NASA engineers to traverse the Martian surface and has been used on every Mars rover as well as other all-terrain robots. The design is composed of two different parts. The bogie is derived from old railway systems. The trains had an undercarriage that was able to curve around the track. On a traditional rocker-bogie system the bogie refers to the first two wheels on the rocker, that are able to swivel independently from the rest of the rocker. The other part of the system in the rocker. The rocker uses a differential bar between the two sides to ensure that the robot remains stabilized. Because of the differential

bar when one side of the robot goes over an obstacle it pushes the rocker down, thus keeping all four wheels on the ground [20]. A diagram of a rocker-bogie robot going over difficult terrain can be seen in Figure 9.

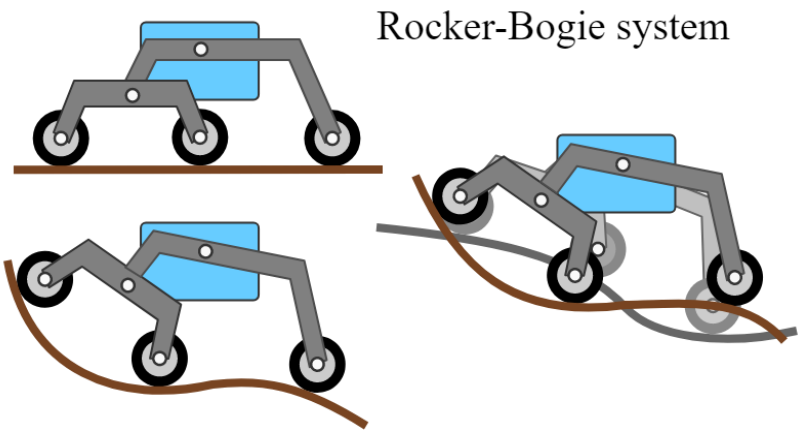

Figure 9: Rocker-Bogie System [21]

While the rocker-bogie system is one of the best robotics systems for traversing rough terrain, the capabilities of the system were far beyond what we needed. While not as complicated as other all-terrain drivetrains, it does present some complications which could add cost and imported materials required for capabilities we do not necessarily need. For these reasons, we felt that the rocker-bogie system did not match AFIA's needs.

The Red-Rover rocker is a rocker-bogie derivative invented by Carnegie Mellon for the Google Lunar X-Prize competition. This rocker utilizes fewer wheels and fewer free rotating axles than the rocker-bogie. These changes decrease the complexity of the Red-Rover rocker in comparison to the traditional rocker-bogie. The four-wheel design does lose some terrain abilities in comparison to the six-wheel rocker-bogie and the skid steering decreases its agility. This agility loss can be overcome by adding four-wheel drive. The design of the Red-Rover does not utilize specialized components, like tread, and, with the exception of the differencing bar, any other part of the system can be removed or repaired without dismantling the entire drivetrain. The four-wheel design features fewer gears and motors than the other systems. Minimizing the amount of expensive components included in the design decreases the overall cost and aligns the Red-

Rover rocker with the sustainable cost goal of the AFIA MQP [9]. At a final weighted score of 199, a Red Rover rocker system was selected for use in AFIA.

3.3 Rocker Design

One of the most important parts of the robot is the rocker, without which the robot would not be able traverse obstacles. For the following modeling exercises we will define theta as the angle between the rocker legs. This is a constant, and once set does not change. We are particularly interested in the angular displacement which will be defined as the angle of the rocker compared to an axis perpendicular to flat ground. A diagram showing our angles can be seen below.

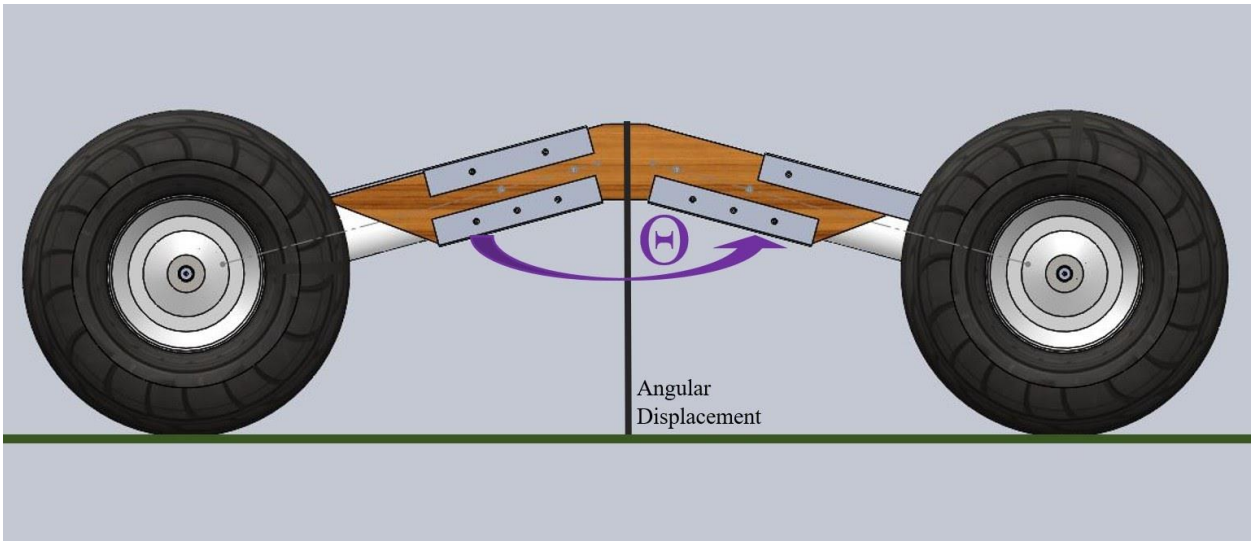

Figure 10: Rocker Angle and Displacement

To understand how the rocker needed to move we created a bond graph to model the movement of the rocker while going over certain obstacles. To model the movement of the robot we used a bond graph which can be seen below in Figure 11.

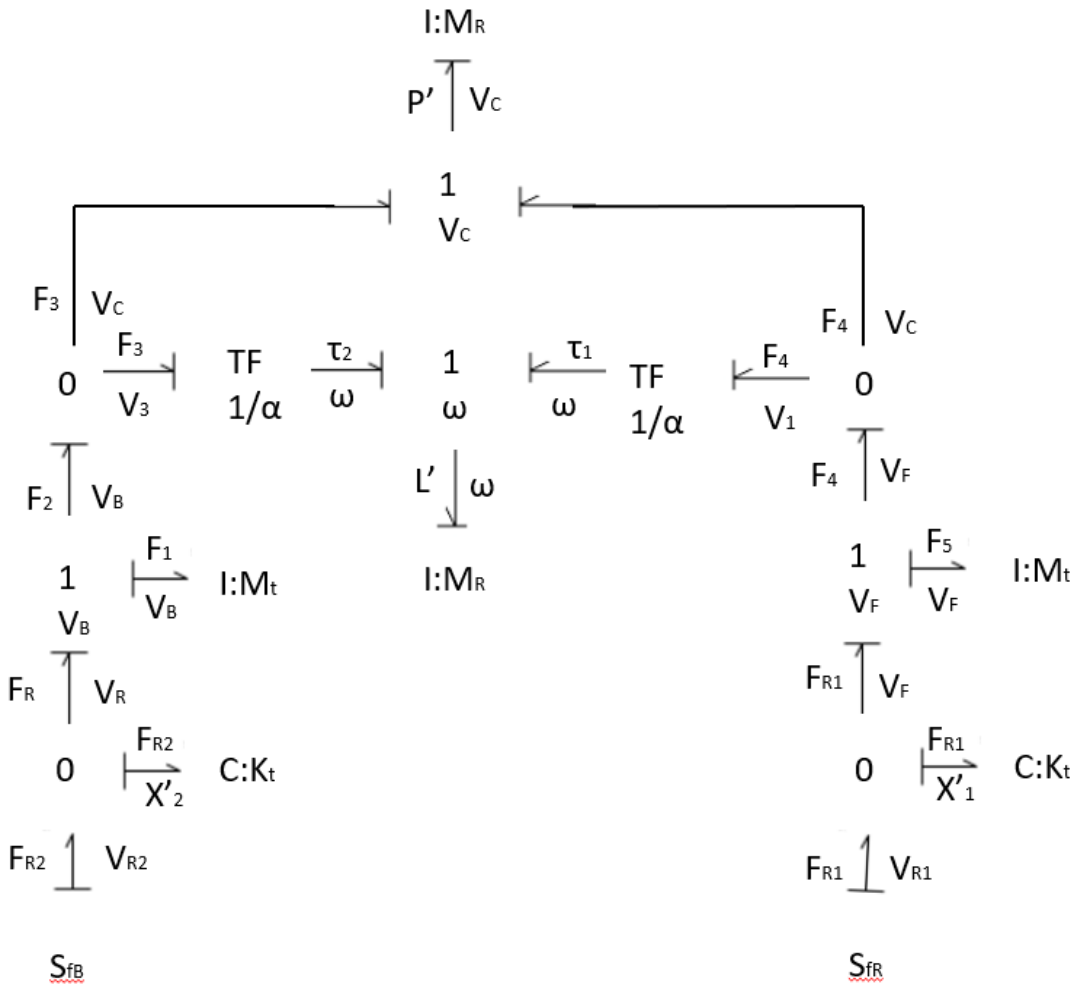

Figure 11: Bond Graph

After we had our bond graph, we were able to derive state equations as seen below in Equation 3.

$$\begin{bmatrix} X_1' \\ X_2' \\ p' \\ h' \end{bmatrix} = \begin{bmatrix} 0 & 0 & \frac{-1}{M_{rocker}} & \frac{1}{L * J_{rocker}} \\ 0 & 0 & \frac{-1}{L * J_{rocker}} & \frac{1}{M_{rocker}} \\ \frac{1 - \frac{1}{J_{rocker}}}{a} * K & \frac{1 - \frac{1}{J_{rocker}}}{a} * K & 0 & 0 \\ \frac{(1-b) * K}{L} & \frac{(1-b) * K}{L} & 0 & 0 \end{bmatrix} * \begin{bmatrix} X_1 \\ X_2 \\ p \\ h \end{bmatrix}$$

Where:

M_{rocker} is the Mass of the rocker

J_{rocker} is the moment of inertia of the rocker

K is the spring constant of the wheels

L is the length of the rocker leg

M_{wheel} is the mass of a wheel

X_1 is the height of the front wheel from the ground

X_2 is the height of the back wheel from the ground

p is the momentum of the rocker

h is the angular momentum of the rocker

$$a = 1 + \frac{1 + M_{wheel}}{M_{rocker}} - \frac{1 + M_{wheel}}{J_{rocker} * M_{rocker}}$$

$$b = \frac{(1 + M_{wheel}) * (1 - \frac{1}{J_{rocker}})}{M_{rocker} * a}$$

(3)

We then used these state equations to model the system. We used MATLAB to solve the equations. Because we wanted to be able to try a lot of different variables, we were mindful to make it as easy as possible to change the variables. We did this by making a rocker class so that we could easily create multiple rockers and test how different dimensions affected the angular displacement. Our goal was to ensure small angular displacements from our defined Z-axis, as represented by the black line in Figure 10. By minimizing rocker angle, we were able to handle larger terrain differences without bottoming out the rocker. We found that the easiest variable to

change was the angle. The results on the same road can be seen for three different angles below in Figure 12.

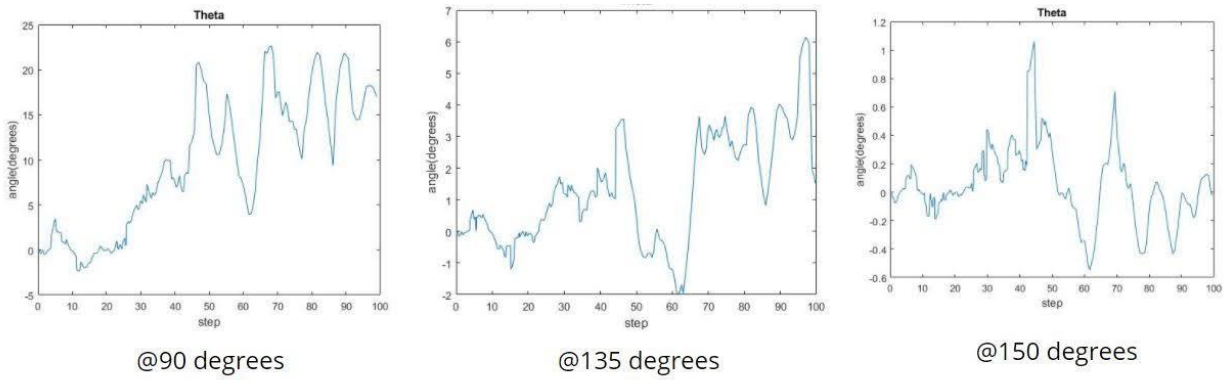

Figure 12: Change in Angle Given Theta

Given our previously discovered dimensions, we have decided to go with a theta of 150 degrees.

The rocker itself is made of PVC, connected with a wooden bracket connecting the two sides of the PVC. The PVC allows us to easily interface with the gearbox and wheels. The wooden bracket also acts as an attachment point to the robot base. The wooden pieces form a box around the PVC. ¼-20 bolts connect the PVC to the wooden bracket. The wooden bracket ensures that the PVC is at a 150-degree angle. The pivot point utilizes Delrin, which has a low friction coefficient, is extremely easy to manufacture, and inexpensive. The ball joint which connects the rocker to the differential bar uses a commercial off the shelf (COTS) ball joint rod end that can be screwed into the wood using a T-nut. The links of the differential bar are made from aluminum tubes with the two COTS ball joints on each side. The differential bar is made from ½-inch thick wood. It is thickest in the middle at the pivot point, where the largest bending moment is located. Like the pivot points on the rocker, the pivot point will be made of Delrin. In Ghana, the differential bar would most likely be made of teak, but for cost considerations, in the States, it may be made out of a less expensive material that is treated to be weatherproof. A render of the rocker system can be seen below.

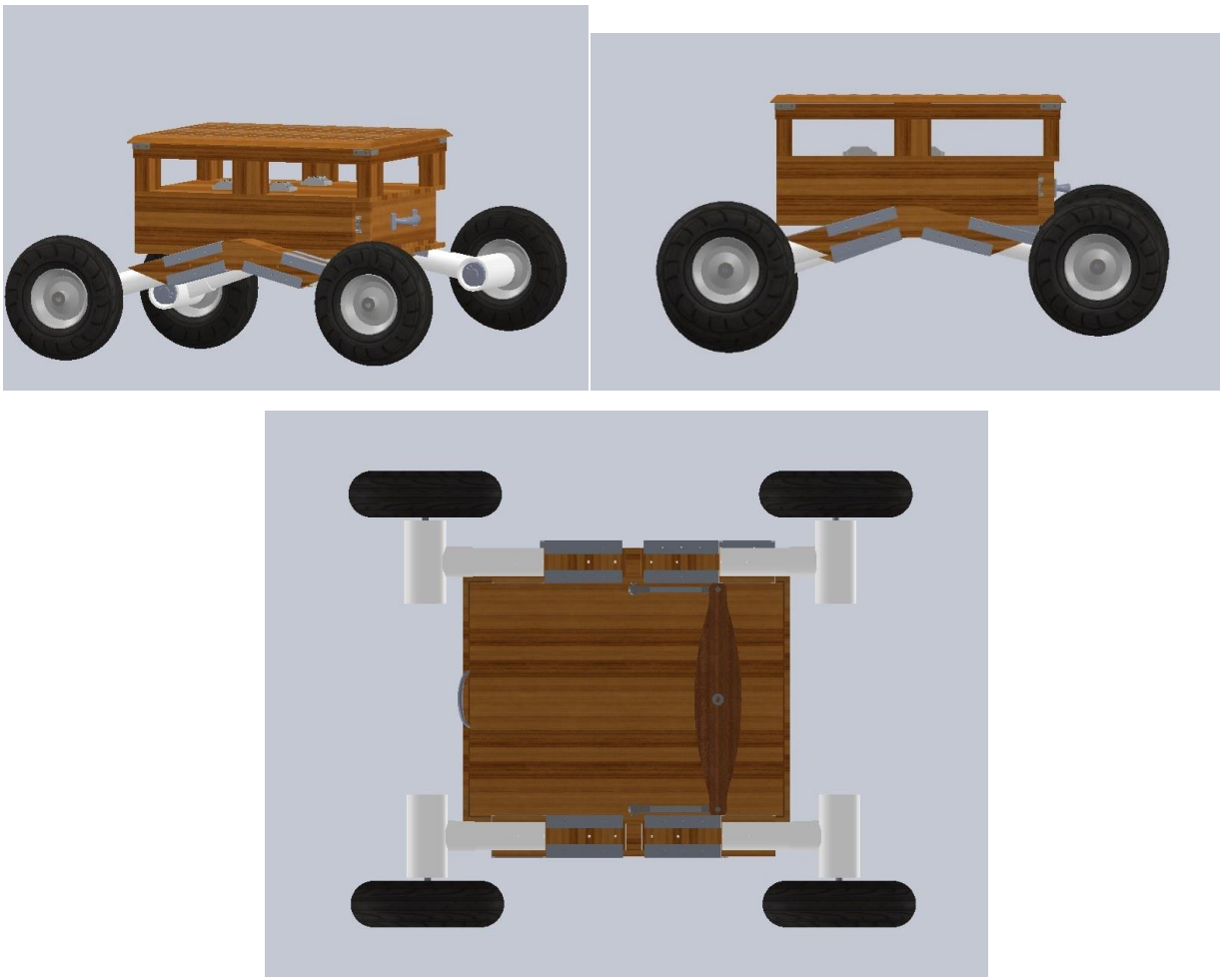

Figure 13: Rocker CAD

3.4 Rocker Prototyping

Prior to building our full robotic system, we built a 1/6th scale model prototype made of LEGO. The LEGO model was run over a variety of terrain to prove the rocker design was capable of stabilizing the chassis during operation. The scale model test also indicated the maximum displacement of the wheels before the rocker system reached its limits. This test revealed that the maximum scale model obstacle size was 3 inches high. This obstacle size is strictly that of the rocker system as the wheels used for driving the scale model were themselves not to scale. Increasing the size of the wheel increased the size of the obstacle that could be overcome.

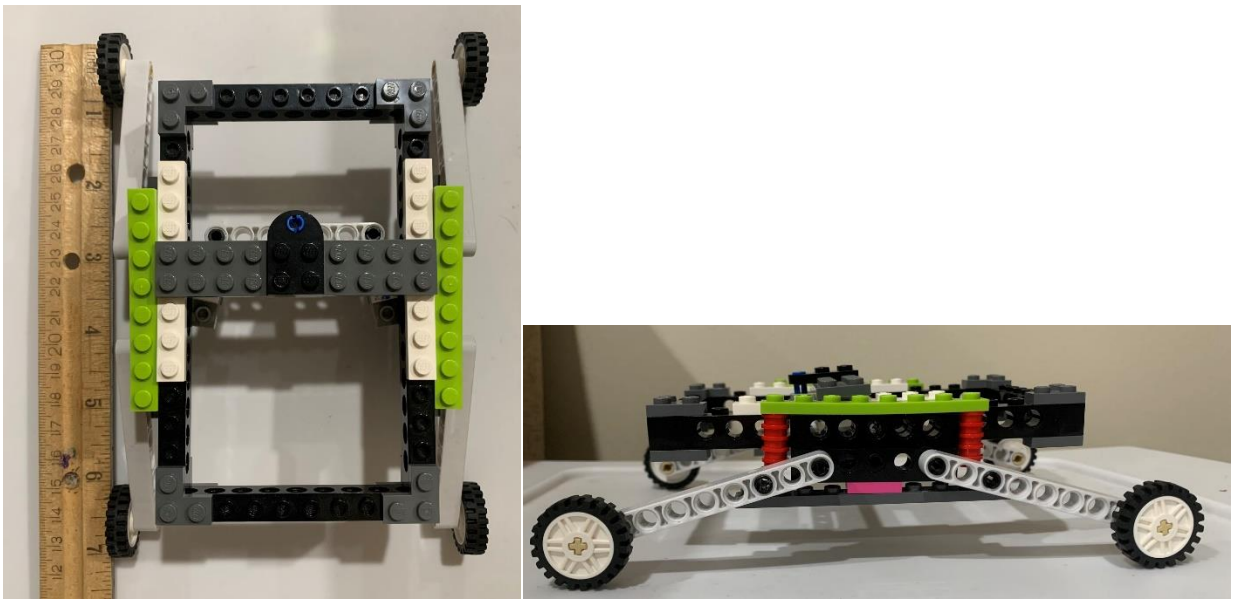

Figure 14: Rocker Scale Model Top and Side Views

3.5 Rocker Construction

3.5.1 PVC

PVC was selected for the construction of the rocker legs because it is readily available in Ghana and most countries and could be solvent welded to form a permanent joint between two fixtures. Solvent welding (more commonly referred to as solvent cementing) involves using a chemical combination of a solvent and cement to fuse two pieces of PVC [22]. The solvent weld ensured that once we attached the rocker legs to the motor holders they would essentially act as one solid piece. Our set-up can be seen below in Figure 15.

Figure 15: PVC Solvent Welding Setup

To attach the PVC to the wooden rocker holders we had to drill holes straight through the PVC. To do this we first drilled a ¼ hole straight through the PVC, and then expanded it with an F-sized drill bit on both sides for clearance.

3.5.2 Brackets and Holders

The brackets and holders were constructed with a mixture of ¼-inch plywood and ½ -inch oak hardwood, cut with a jigsaw and treated with wood stain. The holders, being regular rectangular shapes, were simply measured, marked, and cut out of the plywood. The bracket pieces, however, had more unique and complex designs, and had to be cut with more precision and support. Diagrams of their designs were printed out and taped to the oak, then slowly and carefully sawed out to maintain their precise shapes and angles. Each of these four brackets had four small holes drilled for attachment to the PVC, and the two brackets for the insides of the rocker legs additionally had two holes along the centerline, one above the other; the higher of these holes is for attaching a ⅜-16 t nut, which screw into the shoulder bolts of the rocker pivots; the lower is for attaching a 10-24 t nut, which then fits to the differencing bar.

Figure 16: Bracket and Holder Pieces Staining

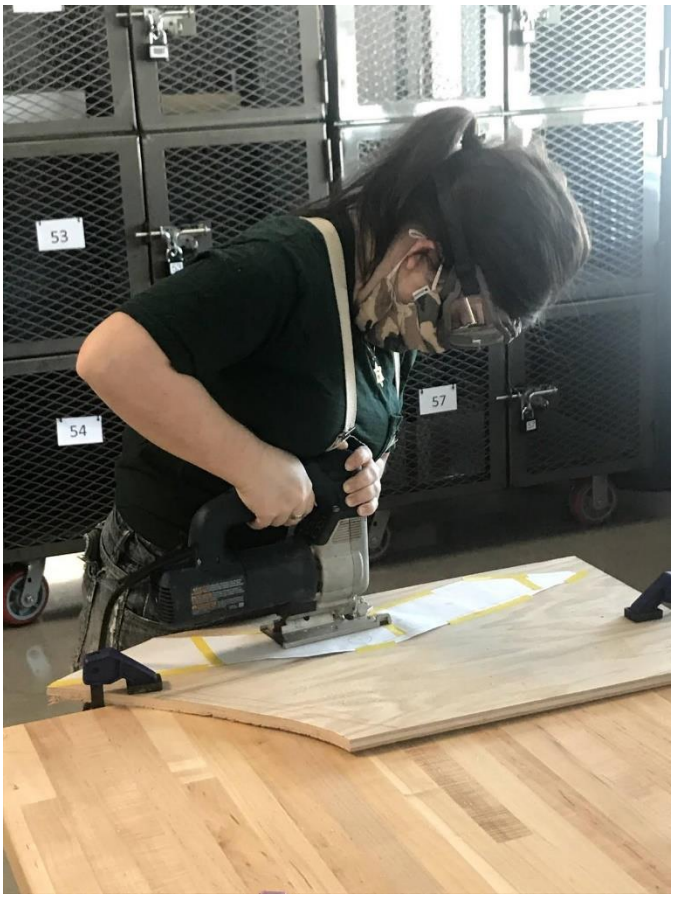

Figure 17: Jig Sawing of Bracket Pieces

3.5.3 Differencing Components

The wooden differencing bar was cut out of the same ½-inch oak as the brackets. It was also stained, and holes were drilled to attach the differencing sides. A shoulder bolt was placed through the middle of the differencing bar to create a pivot point on the underside of the battery drawer.

The AFIA design features ten components that were turned on a CNC lathe, with half of these components used in the rocker system. The Delrin bushings were turned because it was not possible to fixture them securely for manual drilling. The differencing sides were threaded on the lathe. The stock for the differencing sides was ½-inch aluminum; the ends of the stock were cut down and threaded to fit within a female M5 tie rod end.

The most complicated lathe operation was the threading. The rocker could not be assembled without the differencing sides or the Delrin bushings. Once these components were completed, rocker construction moved along smoothly.

3.6 Stress Analysis

PVC was selected for the legs of the rocker based on its availability, variety of fixtures, and the storage potential of hollow tubes. PVC has a low strength-to-weight ratio and is flexible in nature which created concerns about its ability to support the chassis. The maximum force applied to the PVC rocker was calculated and compared to the recorded compressive and tensile strength of PVC to ensure it was a viable material. In order to be conservative about the force applied to the PVC, calculations were performed assuming half the weight of the robot, excluding the rocker weight, was placed on one rocker that was positioned on a 30-degree slope as shown in Figure 18.

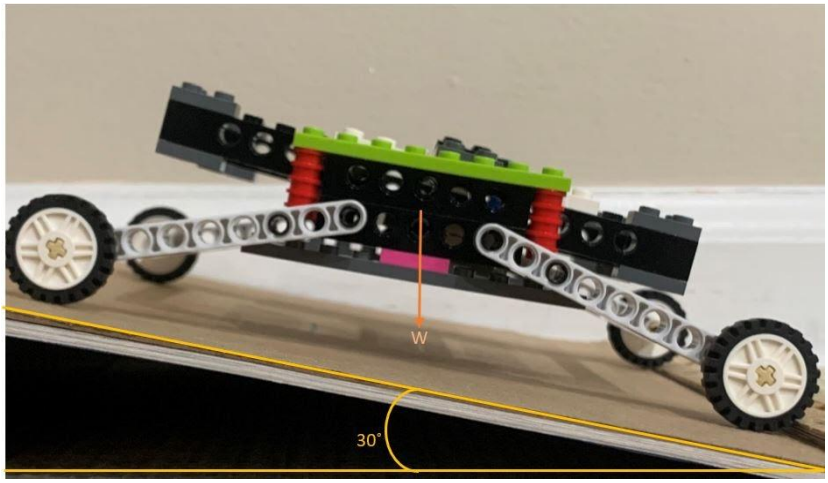

Figure 18: Robot Model on Slope

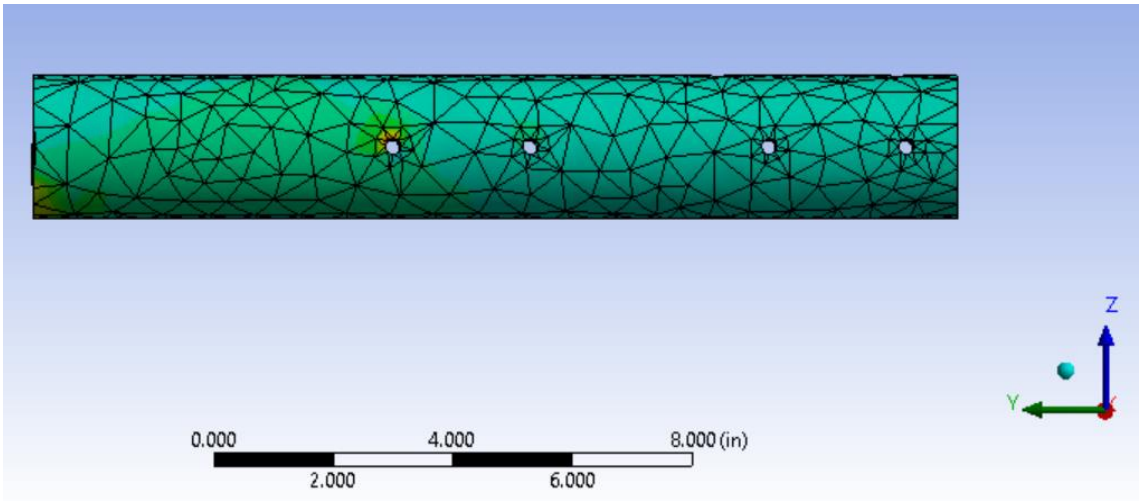

Figure 19: FEA of PVC

This model was analyzed using ANSYS and the stresses produced could then be compared directly to the documented compressive and tensile strength of PVC. It was determined that even with the worst-case scenario loading, there would not be enough force to cause plastic deformation or PVC failure. The maximum tensile stress produced was 2693 psi while the tensile strength of PVC is 7,450 psi. The maximum compressive stress was 1371 psi and compressive strength is 9,600 psi. This loading had a factor of safety of 2.8 for tensile stress and 7 for compressive stress. This comparison showed that PVC was capable of supporting the chassis in the worst-case scenario which made it an acceptable material for the rocker legs.

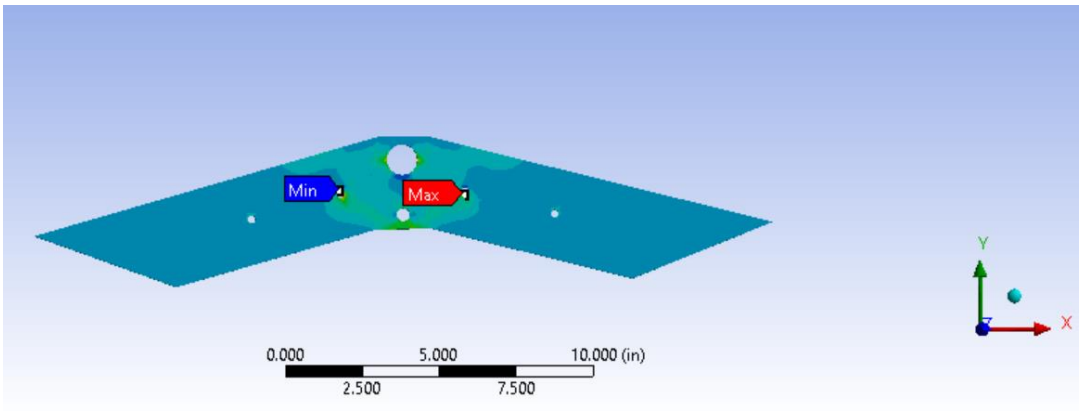

Figure 20: FEA of Wooden Bracket

Another ANSYS simulation was created for the wooden rocker bracket to verify the two brackets were capable of operating under the weight of the robot. With the findings from this simulation, we calculated a compressive safety factor of 54 and a tensile safety factor of 2.75. The maximum compressive and tensile loading occurred around the bolt holes and the rocker mounting holes. The maximum compressive stress was 55 psi and the maximum tensile stress was 280 psi. This loading and safety factor indicated that the bracket was more than capable of supporting the weight of the robot under static loading.

3.7 Wheels

For wheels, we initially elected to go with the 6-inch OD Westcoast Products pneumatic centipede tires. They are durable, have good traction and are relatively inexpensive for our purposes. As a bonus, CAD models of both the tire alone and wheel assembly are available on the site website. But it soon became clear a 6-inch diameter for wheels situated fairly close to the bottom of the chassis meant at worst, a situation we had to keep in mind throughout design, only 3 inches of clearance below the robot body, insufficient for even small rocks and debris. Thus, we switched to standard 13-inch diameter wheelbarrow wheels, necessitating changes in our motor and gearbox sizing but giving a much more reasonable and practical obstacle clearance height. The particular wheels we purchased were from Harbor-Freight and are shown below in Figure 21.

Figure 21: 13-Inch Wheelbarrow Wheel

Since these wheelbarrow wheels were initially free spinning, the bearings had to be removed in order to transfer the torque from the motors to the wheels. These bearings were removed using an arbor press and replaced by hub inserts.

The final turned parts incorporated into the AFIA construction were the wheel hub inserts. These pieces were turned out of a 1 ½-inch diameter aluminum bar. They feature a slight chamfer on the front end to facilitate a simple press fit into the wheel hub and a flange on the back end to prevent the insert from being pressed completely through the hub. The turned part included a half inch hole all the way through. This hole was broached on a manual arbor press with a ½-inch hex broach. The broaching was necessary to allow the wheel to interact with the gearbox. The selected gearbox, discussed in the following section, has a ½-inch hex output shaft. This shaft will engage with the insert and turn the wheel.

3.8 Motor Selection and Gear Ratio Calculation

The first step in motor sizing was to determine the power necessary for the motor to drive on flat ground at the secondary speed goal of 5 mph. For this calculation planetary gearbox efficiency was assumed to be 97% per stage. In order to account for slight sinkage into the soil, flat ground is approximated as a 15-degree slope.

$$P = W * vel * \sin(\theta)$$

$$P = 150lbs * 5mph * \sin(15°) = 368W \tag{4}$$

$$P_{Gross} = \frac{P}{0.97^3} = 423W$$

$$\frac{P_{Gross}}{motor} = \frac{423W}{4\ motors} = \frac{106W}{motor} \tag{5}$$

With the necessary power for travel on flat ground calculated, we began looking for motors that operate around 100 Watts at maximum efficiency. We focused primarily on robotics competition motors as they are cheap, durable, and appropriate for the desired size of the robot. The three motors investigated were the CIM, the Mini-CIM, and the CCL 9015 (RS-500 series). Of these motors, the CIM most closely fit the necessary power for the robot.

Next, we calculated the output torque necessary to drive on flat ground. The torque required to drive the robot up a 15-degree slope, our approximation of flat ground, was determined using Equation 6 below. The angle was then changed to 45 degrees, the maximum slope accounting for a 15-degree flat ground slope, and output torque was recomputed.

$$T = W * r * \sin(\theta)$$

$$T = 150lbs * 6.5in * \sin(15°) = 252\text{inlbf}$$

$$T_{Gross} = \frac{T}{0.97^3} = 276inlbf$$

$$\frac{T_{Gross}}{motor} = \frac{276inlbf}{4\ motors} = \frac{69inlbf}{motor}$$

$$T = 150lbs * 6.5in * \sin(45°) = 689inlbf$$

$$T_{Gross} = \frac{T}{0.97^3} = 755inlbf$$

$$\frac{T_{Gross}}{motor} = \frac{755inlbf}{4\ motors} = \frac{189inlbf}{motor} \quad (6)$$

The gear ratio was based on the maximum slope torque. This maximum torque was calculated accounting for a 3% efficiency loss per stage. This equation, accounting for torque, is seen above is Equation 6. The torque necessary to drive up the maximum slope was divided by the input torque of the motor when operating at 25 amps. This ensures that the robot will be capable of overcoming the maximum slope. The resulting gear ratio was 43:1 which was rounded to the more standard 48:1. The gear ratio was then used to validate the flat ground travel speed met at least the primary goal of four miles per hour.

$$Gr = \frac{Tout}{Tin}$$

$$Gr = \frac{186inlbf}{4.4inlbf} = 43 \quad (7)$$

$$Speed = \frac{\omega_{motor}}{Gr} * C_{wheel}$$

$$Speed = \frac{5000RPM}{48} * 40.82in = 4.03\frac{mi}{hr} \quad (8)$$

Due to the PVC rocker leg system, any gearbox must fit within a PVC T-fixture. In order to minimize the size and complexity of the gearbox, planetary gears were selected. Due to the

standard nature of the desired gear ratio, COTS planetary gearboxes were researched. Two gearboxes were available, the CIM Sport gearbox and the VEX Versaplanetary gearbox. Both are compatible with the CIM motor. The CIM Sport gearbox was selected based on cost. The VEX Versaplanetary gearbox required an adapter to interface with the CIM motor and had a higher cost overall. Since AFIA is supposed to be a cost-efficient robot and both gearboxes come with a ratio of 48/1 the cheaper gearbox was used.

The CIM motors and gearboxes needed to be held in place within the PVC T fixture. This was accomplished using two 3D printed components. The first piece has a square hole that fits around the CIM Sport planetary gearbox. Eight bolts were placed through the PVC and PLA. They bolted into holes on the sides of the gearbox. The motors, on the other hand, did not have any bolt holes. The motors were supported at the back end by a PLA ring. These supports were bolted to the PVC behind the motors as there was not space to place a bolt or nut between the motors and the PVC.

3.9 Batteries

The AFIA battery selection process began with a comparison of lithium-iron, lithium-ion, and lead acid batteries. Preliminary research utilized 12V, 100Ah batteries to compare cost and weight. The comparison, shown in Table 5, indicated that lead acid batteries are the most cost-efficient battery option, but they weigh significantly more than either lithium-ion or lithium-iron batteries. The data in Table 5 comes from market research on available 12V 100Ah batteries.

Category	Lead Acid [23, 24, 25]	Lithium Iron [26, 27]	Lithium Ion [28]
Capacity (Amp Hours)	100 Ah	100 Ah	100 Ah
Nominal Voltage	12 V	12 V	12 V
Weight	71.5 lbs	26.4 lbs	32 lbs
Approximate Cost	$200	$500 - $700	$800 - $1000

Table 5: Battery Comparison Research

After researching baseline differences between the three main battery types, the specific battery needs for AFIA were calculated. The necessary voltage was determined to be 12V based off the voltage necessary to run the drive motors. The nominal output current was determined using the previous flat ground power calculation and a motor table for the CIM that correlates power to current. This determined amp-hours is for operation on flat ground; it was doubled to find the amp-hours necessary to meet the two-hour battery life goal.

With the necessary battery parameters found, specific batteries were investigated. Three types of batteries were researched: motorcycle batteries, go-kart batteries, and multipurpose lithium-iron batteries. First, the number of batteries necessary to achieve the required battery parameters was calculated. From here, the total weight and cost of the batteries was calculated. The results of the calculations are shown below in Table 6. During our market research we were unable to find a lithium-ion battery that met the specific needs of the AFIA project. One 12V 100Ah battery was prohibitively expensive. The cost-effective lithium-ion battery choice would have required the team to wire 100 AA sized batteries in series and parallel to achieve our voltage and current needs. This option, while feasible from a cost standpoint, was impractical to implement. The lithium-iron battery shown in the table below was the most cost-effective lithium option. As shown in Table 6, the cost of lithium-iron batteries varies greatly by manufacturer and purchase location. Seven lower current batteries from Miady were more cost effective than one 100 Ah battery from Miady or any other brand.

Battery	Type	Volts per Battery	Amp Hours per Battery	Number Necessary	Overall Cost	Overall Weight
Miady [29]	Lithium Iron	12 V	16 Ah	7	$378	27.79 lb
Go-Kart [30]	Lead Acid	12 V	3.5 Ah	30	$450	95.1 lb
Motorcycle [31]	Lead Acid	12 V	22 Ah	5	$250	78.4 lb

Table 6: Summary of Battery Calculation Results

From the calculation it was determined that the best option for the AFIA robot was lithium-iron batteries. While seven of them are necessary to run the drive motors, these batteries were approximately one third the weight of the necessary lead acid batteries and a better fit for the chassis interior than the larger lead acid batteries.

3.10 Box Design

The main goal of the box design was to allow for maximum storage space while being versatile and ensuring that all parts of the box have easy access as well as an electronics area with an IP54. To accomplish this, we divided the box into three different sections: the battery drawer, the electronics box, and the lid.

Figure 22: Box CAD

3.10.1 Battery Drawer

The bottom-most layer of the box in the battery drawer. With the given battery selection, to house all seven batteries, almost an entire level had to be devoted to the batteries. To accomplish this, we will be using standard 24-inch drawer sliders to allow easy access to the battery drawer. To ensure that the batteries cannot move around once they are inserted into the robot, we will be

using laser cut custom holders. This battery drawer has room for nine separate batteries which can add half an hour of battery life to the anticipated 2 hours or act as back up batteries.

3.10.2 Electronics Box

Above the battery drawer is the electronics box. The electronics box has beeswax cloth along the outside. Beeswax cloth was originally created as an environmentally conscious way to preserve food, that could be easily created with household supplies. We will be using it as a way to keep water and dirt out. A fan cooling system will help ensure that the electronics do not overheat, and will be discussed later.

3.10.3 Lid

The lid is designed to lift up to allow for easy access to the electronics box below. It has a standard bolting pattern of over one hundred 10-24 t-nuts. The holes in the lid that accommodate this bolting pattern are secured against water ingress via attachment of beeswax cloth.

3.11 Box Construction

The drawer, box, and lid were all constructed of plywood, fixtured together using wood screws and reinforced with wood glue, and all treated with outdoor grade wood stain. All screw holes were first pre-drilled, to ensure correct placement and prevent splitting of the wood, especially on the thinner wood. The exterior of the drawer had pine 2x6 sides. The top of the lid, interior of the drawer, and bottoms of the electronics box and drawer exterior were all made of ½-inch thick plywood. The sides of the lid were made of ¼-inch thick plywood. The sides of the electronics box were made of pine 2x4 board. The sides of the lid, interior of the battery drawer, and drawer handle were all secured with ¾-inch #8 wood screws; everything else unless otherwise specified was secured with 1 ½-inch #10 wood screws.

3.11.1 Battery Drawer Construction

The battery drawer exterior consists of a bottom rectangular board with three framing sides secured to it by drilling up into it through said bottom board, then secured to one another at their corners drilling into the broad side of one board along the length of the next. The stationary components of the drawer sliders were then affixed to the insides of the longer two framing sides using the short screws that came with the slider kit for this purpose. The drawer interior has a similar design, four sides fixed to one another at the corners and to the bottom by drilling up into the siding. One of the short sides, the front, has a metal handle fixed to its center so the battery drawer can be pulled out easily. The mobile components of the drawer sliders are fixed to the exterior of its long sides with the slider kit screws. The two drawer boxes slide together, with the smaller box sitting comfortably within the larger. It pulls out smoothly but with some resistance, stopping the battery drawer from simply sliding out anytime the robot is pointed downhill.

Figure 23: Battery Drawer Construction

3.11.2 Electronics Box Construction

Atop the battery drawer is attached the electronics box. Like the drawer, its basic shape is a plywood bottom with sides attached by drilling into them through the bottom. Rather than sides made of plywood forming a rectangular prism, however, its sides are six short blocks of 2x4, one

at each corner and one at each midpoint of the long sides. A long strip of beeswax cloth for weatherproofing coming up most of the height of these side blocks and going along the entire box perimeter is secured to these blocks using standard office staples. The remaining clearance has breathable air filtering likewise stapled along the perimeter to keep out dust and debris while allowing the electronics to vent heat.

Figure 24: Electronics Box

3.11.3 Lid Construction

Finally, atop the electronics box sits the lid. It fits with a comfortable clearance for easy removal. The sides, in addition to being screwed together with ¾-inch #8, are secured at the corners with corner brackets, the flat tops of which are drilled up through to secure on the top. The excess length of the screws was dremeled off to remove the protruding sharpness. Finally, 130 holes were drilled in a 10x13 grid to form a standard bolting pattern, each with a 10-24 t-nut, for future fixturing of additional components.

3.12 Cooling System

One concern of the AFIA mission scenario was operation in the Ghanaian climate, which meant that even in the cooler parts of the country the robot would need to be able to function in 90 degrees Fahrenheit weather. The sensors selected to detect ditches and obstacles were rated for operation in temperatures up to 140 degrees Fahrenheit. These were placed outside the chassis and were thus only subject to the ambient air temperature. Based on Ghanaian climate data the sensors were capable of operating safely. The Arduino and Raspberry Pi were rated for temperatures up to 180 degrees Fahrenheit. This seemed like a safe operating range, but the electronics were mounted inside the wooden chassis where temperatures could potentially exceed the ambient air temperature. In order to ensure the safe operation of the electronics, steps were taken to reduce thermal barriers in the chassis and a forced convection system was implemented.

To determine how much forced convection was required, we had to first determine the heat produced by the electronics in the box. We assumed that all the power from the boards is converted to heat, and the SPARK motor controllers are 95% efficient. The heat produced can be found in Table 7 below. All voltages and amps are derived from official documentation. For the Sparks we are using the continuous current [32].

Component	Voltage (V)	Current (A)	ineffciency	Watts (all converted to Heat)	# of components
Raspberry Pi	5	1.2	1	6	1
Arduino	5	0.08	1	0.4	1
Spark	12	60	0.05	36	4
Temp Sensors	5	0.001	1	0.005	2
		Q_produced =		150.41	W
Q_produced =	150.41				

Table 7: Heat Produced by Electronics

From this we were able to calculate air flow required to keep our electronics from overheating using Equation 9 below [33].

$$Q = \frac{178.4 t_i q}{\Delta T P_b}$$

(9)

Where:

t_i = inlet temperature in Rankins

q = power dissipated in kW

ΔT = change in temperature

P_b = barometric pressure at the air inlet

Q = air flow required in CFM

For our inside temperature we used 170 degrees Fahrenheit, as we wanted a bit of safety between the temperature inside of the box and the maximum operating temperature for the electronics. Table 8 shows the air flow required for our primary, secondary, and tertiary goals.

Outside Temperature	**CFM Required (no impedance)**
90 F	6.15
100 F	7.16
110 F	8.50

Table 8: CFM Required Given Outside Temperature

Because fans are likely to experience impedance, the fans purchased for AFIA produced higher CFM then required to ensure the electronics do not overheat. The CFM required with impedance is higher than that of an average computer fan, so we will have two fans in parallel.

The fans were run continuously while the robot was operating. Since computer fans were selected, the current necessary to run the fans was minimal and the fans were capable of long-term operation. Rather than controlling the cooling system, the temperature sensors were used as a failsafe to disable robot operation if the internal temperature exceeded the safe operating temperature.

We chose to utilize two fans rated at 38 CFM to account for additional electronics that may be added to the electronics box in future iterations. The placement of the box can be seen below in Figure 25.

Figure 25: Fans in Box

Another aspect of AFIA's cooling system is beeswax treated cloth around the sides of the electronic box instead of the wooden siding featured in the rest of the robot. First, a lightweight cotton fabric was treated with beeswax, making it water resistant while still allowing air to flow through the fabric. This fabric was less insulative than the wood used for the chassis, thus the electronics box was designed with open sides to minimize the wood used. The openings were covered with the beeswax fabric, so the electronics were protected from water and dust. This decreased the overall insulative properties of the chassis.

3.13 Board Selection

The most thoroughly researched electronic component was the microcontroller that would run the robot code. This controller had to not only run the code and operate the sensors but also allow for future sensor integration. This means that a high premium was placed on processor power, interrupt pins, and memory. These categories were given a weight of five as they directly relate to AFIA's multipurpose and expandable goal. Without adequate processing power, memory, and interrupt pins additional sensors could not be easily added to the AFIA platform. Additional processors would be necessary or current components would need to be removed to make space. Other factors considered include cost, the total number of pins, and a board's means of communicating with other boards and controllers. With a weight of four, the previously listed categories were important for operation and testing of AFIA. One of the main goals of AFIA was to minimize the cost of building a robot. Even without accounting for the import costs implied by the mission scenario, the processor is potentially the single most expensive electronic component. Minimizing the cost of the processor while ensuring quality went a long way to keeping the AFIA robot low cost and adaptable. The total number of pins and the means of communication impact both the adaptability and testing of AFIA. Specifically, within the mission scenario, AFIA will potentially need to communicate over a large distance. This was not a goal of the project, but an important consideration for future adaptations. The least important component researched was the availability and quality of the documentation for the board. This was weighted as a one but good documentation could be the difference between simple component integration and challenging integration. The important criteria were placed in a decision matrix and the team gave a score to every component. The total score for each microprocessor or microcontroller indicated the best microprocessor for the AFIA robot.

	Processor Power	Memory	Documentation	Communication	Cost	Number of Pins	Interupt Pin Availability	
Weighting	5	5	1	4	4	4	5	Total
Arduino Mega	2	2	8	4	9	7	1	113
Teensie 4.1	7	5	2	7	6	4	4	150
Teensie 3.X	6	4	2	7	5	6	6	154
Raspberry Pi 3 B+	9	7	8	9	4	4	4	176
Raspberry Pi 4 B	10	10	8	9	3	4	4	192
ESP32	5	3	5	8	10	4	3	148

Table 9: Board Selection Decision Matrix

Based on the decision matrix, the Raspberry Pi 4B was selected as the AFIA microprocessor. It was chosen for its processing power, memory, and ability to run the code off the board. The Raspberry Pi 4B also had the best growth potential as it could be used to control up to four other boards and had a designated camera-input should vision be desired in the future. Research and previous experience indicated that the Raspberry Pi GPIO ports were more prone to damage and shorting than those of the Arduino Mega. This was remedied by connecting the Raspberry Pi 4B to an Arduino Mega. The Raspberry Pi 4B is a microprocessor that can be used to run code on an Arduino Mega microcontroller using built-in USB ports.

Connecting the microcontroller and microprocessor not only increased the reliability of the GPIO pins but also the total number of pins and the overall memory. With this setup, the Raspberry Pi 4B was able to run the main code while the Arduino Mega focused on sensor integration. The Raspberry Pi 4B can be connected to other microcontrollers in the future, should more GPIO pins be necessary. This increased the number of sensors capable of being added in the future.

3.14 Sensor Selection

The AFIA robotic platform had to be able to detect three main concerns: ditches, debris, and the temperature of the Arduino and Raspberry Pi. The electronics temperature was detected using a silicon bandgap sensor. The DS18B20 silicon bandgap temperature sensor is a digital sensor capable of detecting a temperature change of one-degree Fahrenheit. The detected temperature is converted from a digital reading on the chip and returned in degrees Celsius. The code then converted the temperature to Fahrenheit, so the project consistently utilized US Customary units. Monitoring the Arduino and Raspberry Pi will ensure the components are not damaged by excessively high operating temperatures and facilitate testing the cooling system. Three temperature sensors will be used for testing though only one will be used in the operational code. The sensor used in the final code was placed between the Arduino and Raspberry Pi to detect their temperature. The testing sensors were placed on the edge of the box interior and outside the box. These allowed for the temperature to be easily recorded for while testing the cooling system. The efficiency of the cooling system was based on the volume of air pushed through the box and the difference in temperature of the air and electronics.

Ditch and debris detection were crucial to the success of the augmented autonomy system. Due to the mobile nature of the rocker chassis, the placement of the sensors was very important, especially because two sensors of the same kind could result in interference. After researching distance and obstacle sensors for cost and operation, the Sharp Infrared Range Finder was selected for ditch detection while the LV-MaxSonar-EZ 1 Ultrasonic Maxbotix sensor was selected for debris detection. Since the sensors use two different methods of detection there was no concern with their signals interfering when the chassis moved. The debris detection sensor was placed on the chassis while the ditch detection sensors were placed on the rocker legs and aimed ahead of the front wheels.

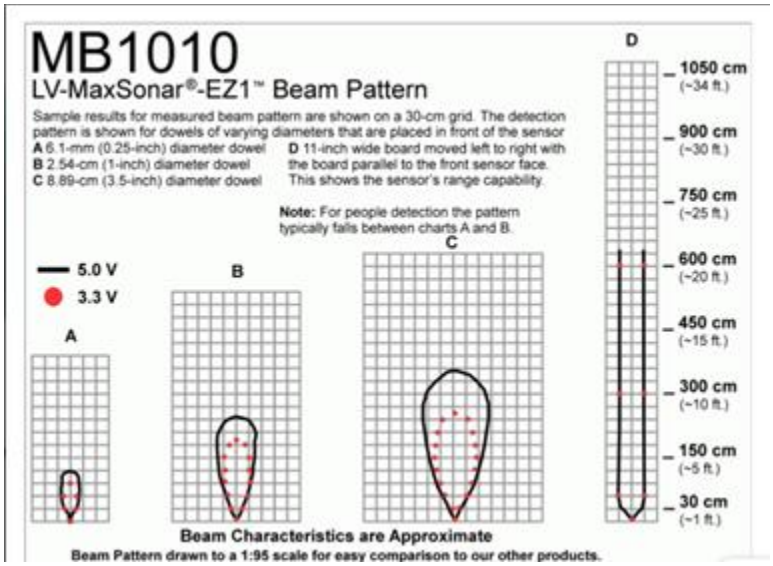

Figure 26: Range Diagram for the Ultrasonic Sensor [34]

The LV-MaxSonar-EZ 1 Ultrasonic Maxbotix sensor was capable of detecting objects between 1 foot and 20 feet away. At the maximum distance, any obstacle larger than 11 inches wide would be detected while at the minimum distance obstacles larger than a quarter inch wide would be detected. AFIA will be able to stop well within the sensor range so it will be able to detect obstacles smaller than one foot wide. The sensor will be placed on the lower front of the chassis, slightly below the maximum safe obstacle height. Since the ultrasonic sensor cannot detect the size of an obstacle, just the distance to the obstacle, the sensor must be placed to only detect obstacles that cannot be overcome. This allows the code to simply stop the motors whenever an

obstacle is detected close to the robot removing the additional step of determining if the obstacle can be overcome or not.

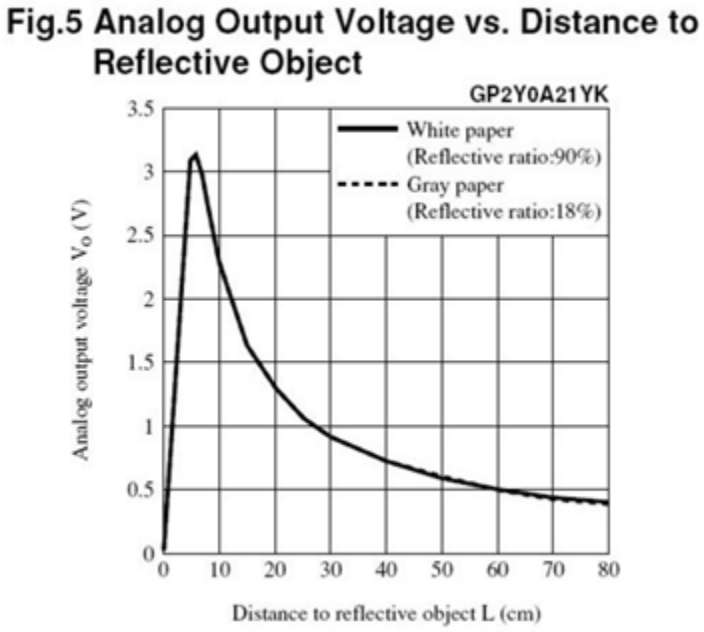

Figure 27: Range Diagram for the Infrared Range Finder [35]

The Sharp Infrared Range Finder was capable of detecting objects up to 2.5 feet away from the robot. These sensors were placed aiming towards the ground in front of the forward wheels. They were attached to the legs of the robot to ensure that chassis motion did not interfere with the distance they detected. These sensors were calibrated by determining the distance from the mounting point to flat ground and the acceptable ditch depth. The readings were then standardized so the result was the distance from the wheel to the ground ahead of the wheel. The readings from these sensors were disregarded if they were less than the acceptable ditch depth. As soon as the range detected exceeded the acceptable depth the robot was stopped. This stopping depth corresponds to the maximum ditch that the robot could drive through. Two sensors were necessary as the rocker-bogie system allowed for either side of the chassis to rotate. This means that one wheel could go into a ditch while the other wheel was on flat ground. In order to avoid bottoming out the rocker or destabilizing the robot, the ground in front of both wheels had to be detected separately. If either wheel encountered a ditch that was too deep the entire robot stopped.

3.15 Teleoperation Control

In order to facilitate testing, AFIA included line of sight teleoperation control. This was done using an RC airplane transmitter and receiver. An RC controller was selected for its increased range and reliability, compared to Bluetooth or wireless internet systems. The HotRC KT-A receiver and transmitter, used on AFIA, had a range of one quarter mile which was more than sufficient for line-of-sight testing. It used a 2.4 GHz signal and had six channels. Three of these channels were used to control AFIA; two were for the tank drive system while the third was an override of the augmented autonomy system. This override was necessary to allow an operator to continue driving the robot after the obstacle avoidance system forced the robot to stop. The additional channels were allocated space on the PCB to facilitate future use.

3.16 Board Layout

To allow for easy connections we created a shield for the Arduino Mega. The shield will use Molex 3 pin connectors to allow for standard connections for sensors as well as for PWM for Motors and RC control. In addition to the previously mentioned sensors, there is room for 13 additional sensors and 6 PWM ports for motor controllers including the 4 drive motors, and 6 ports for RC control. After first reading the documentation, we were under the impression that the Sparks PWM required 6 Volts to trigger, so we used a Step-up Voltage Convertor from Pololu to step up the signal from the 5 Volts from the Arduino to 9 Volts. The schematic can be seen below in Figure 28.

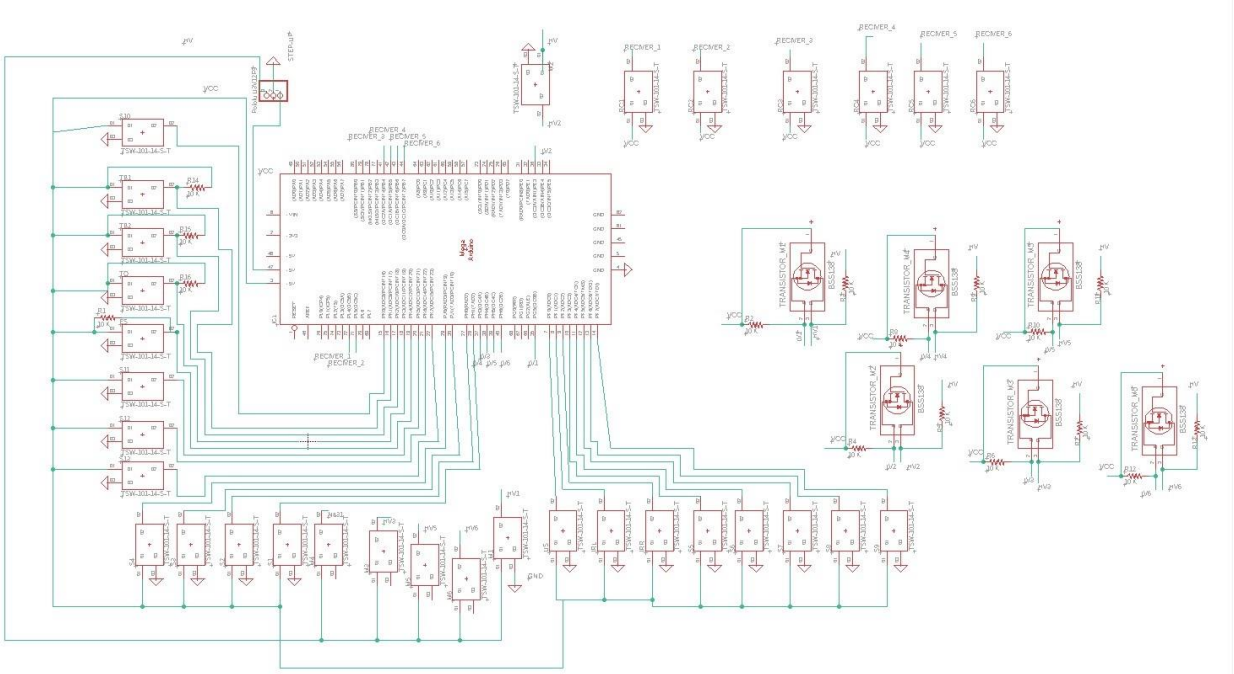

Figure 28: Eagle Shield Schematic

The shield is a 4-layer board, with a 5V VCC and a Ground layer in the middle, and traces on both the top and the bottom of the board. The finished PCB can be seen below in Figure 29.

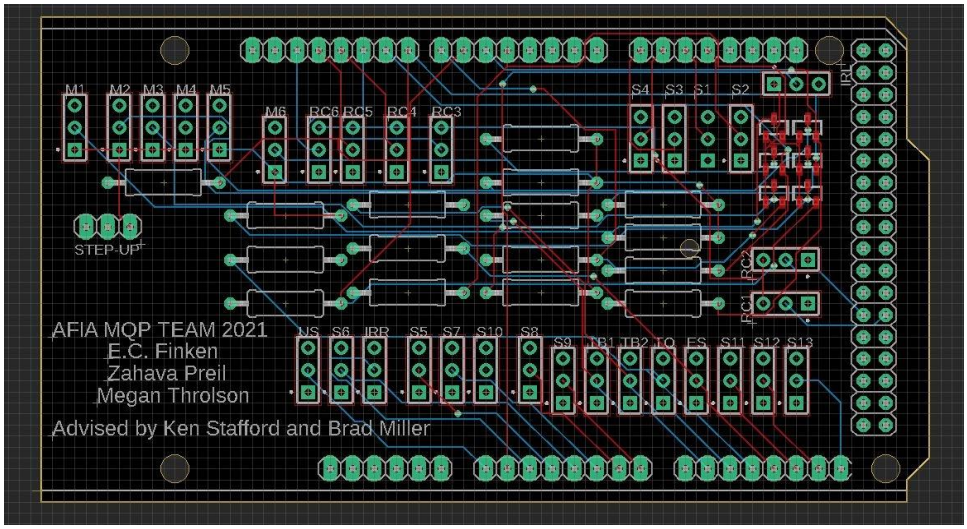

Figure 29: PCB Layout

Once completed Gerber and drill files were sent to JCL PCB in China for manufacturing. By doing this we were able to get five custom boards without any components. The rendering from the Gerber files may be seen below in Figure 30.

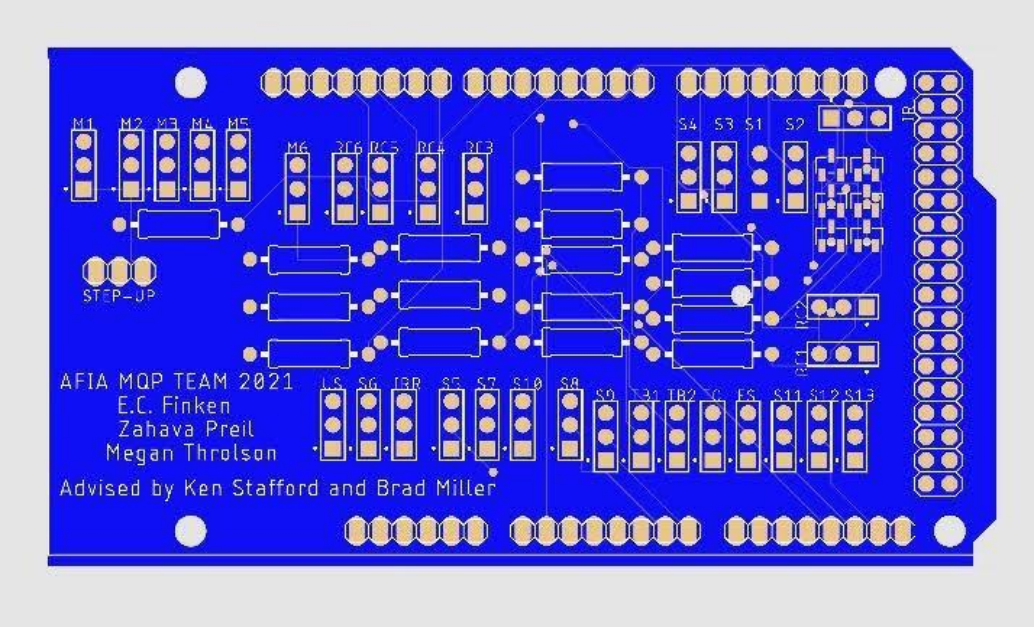

Figure 30: Gerber File Rendering

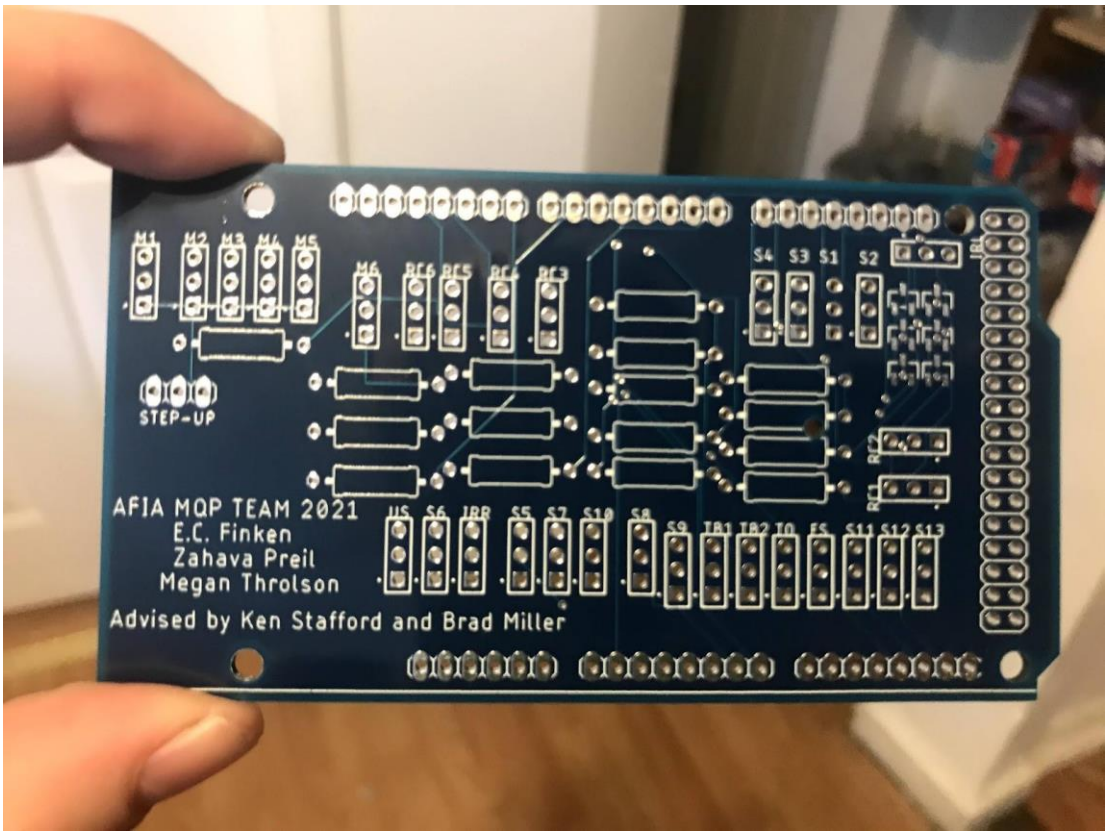

Figure 31: PCB (No Components)

After receiving the board, it was discovered that many of the terminals were not connected to ground, causing the board to be unusable. It was also discovered that the required PWM voltages was not 6 volts, and that the required 6V was to trigger the motor. Because of shifting priorities, we decided to move to using a breadboard for this iteration of the project.

3.17 Code Design

The AFIA robot utilized augmented autonomy with teleoperation controls.
Sensors were key to this. Sensor classes were organized in the code based on what was being measured. Any of the sensors previously mentioned as well as an e-stop button were capable of halting robot operation. The teleoperation controls were disabled until the operator pressed an override button. This teleoperation was impractical when viewed through the lens of the AFIA mission scenario but was crucial to the success of the MQP. The deliverable of this project was a robot made of alternative materials that was sturdy enough to traverse rough terrain and flexible enough to be modified for multiple missions. Teleoperation simplified testing and placed the focus on the robot design while the augmented autonomy laid the foundation for a fully autonomous system. This future development was facilitated in the code through the creation of a sensor superclass, shown below in Figure 32. The goal was to make it simple to integrate new sensors in the code as well as physically.

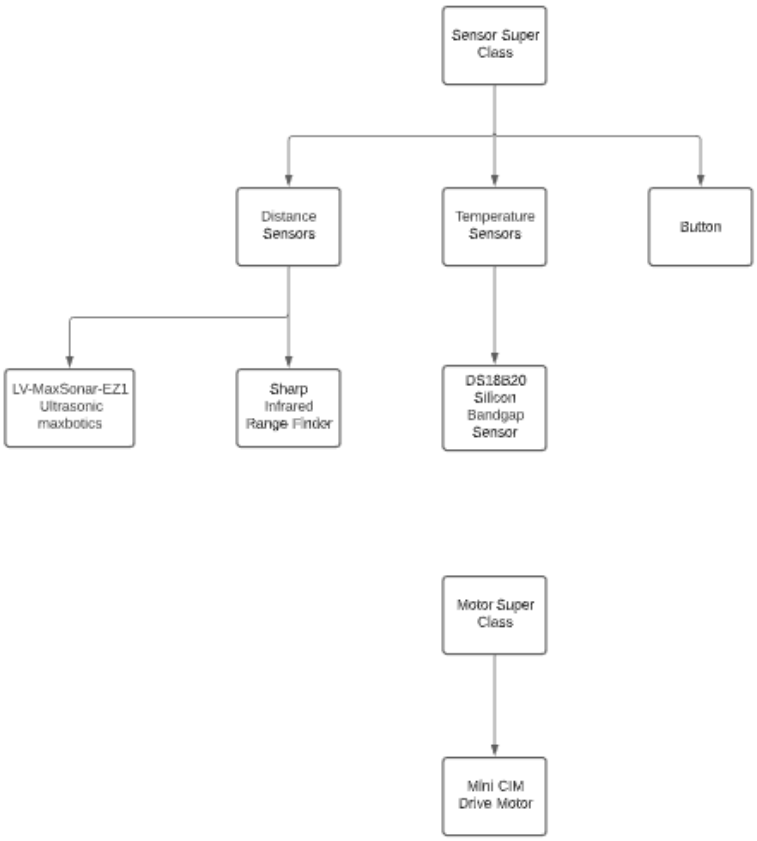

Figure 32: Class Diagram

A state diagram was created to outline the general operation of the robot. This diagram is shown below in Figure 33. The default state for the robot during operation was the drive state. In the drive state, the robot frequently polled the sensors and controller. If the sensors detected a hazard, the augmented autonomy forced the robot into the E-stop state. From this state, the operator had to manually override the e-stop to return to the drive state. If the controller polling returned a new motion command, the robot altered its motion accordingly and passed back into the drive state.

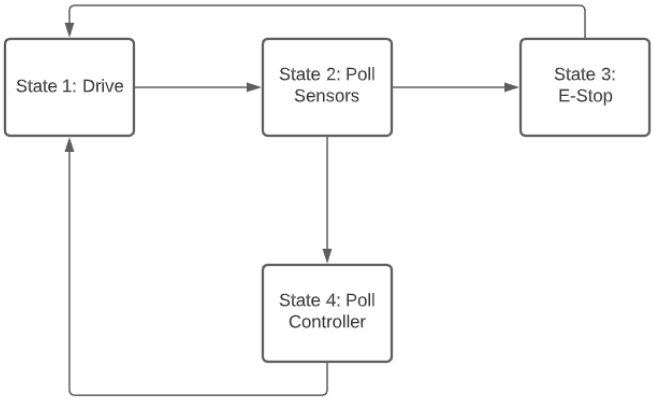

Figure 33: State Diagram

3.18 Code Implementation

To program the Raspberry Pi, we utilized a virtual desktop accessed over Wi-Fi. The code was written using the Arduino IDE on the Raspberry Pi. Using the Pi to program and control the Arduino increased the growth potential of AFIA by allowing for more complicated code and sensor integration in the future. The Arduino and Raspberry Pi interfaced using a USB connection, this way information could be transmitted between the Arduino and Pi. The teleoperation code was standard for robotic control. A pulse was received by the RC receiver and transmitted to a pin on the Arduino based on which channel it was sent on. The Arduino read the duration of the signal using the *PulseIn()* function. This pulse duration was then mapped to a motor value between 0 and 180 where 0 was full reverse, 90 was stopped, and 180 was full forward. In order to ensure the motors stopped correctly, any value between 80 and 100 was set to 90. These values were then converted into a PWM signal and sent to the appropriate motor controller.

4. Results

4.1 Size Goal

The size constraints for AFIA, as outlined in our goals table (Table 2), were based on the trunk measurements of a midsize car, for ease of transport in case of breakdown. This means no component of the robot could exceed 4 feet by 2.5 feet by 2.5 feet in travel configuration, that being the rocker removed from the box and the wheels off the rocker. The wheels themselves are 13-inch diameter wheelbarrow wheels; the rocker was 42 inches long, 22 inches wide, and 11 inches tall; and the box was 12 by 26 by 19 inches cubed, so in travel configuration, AFIA's size goal is neatly met. In addition, disassembly into this configuration was swift and simple, doable by a team of two without specialized engineering knowledge or uncommon tools.

4.2 Travel Speed

The speed of AFIA was calculated by timing the robot as it drove along a set distance and converting that time into miles per hour. Before performing the speed trial, the robot was weighted with bricks to account for the weight of the five missing batteries. The overall robot speed calculation can be seen in Equation 10. Based on the trials and calculations, AFIA drives on flat ground at a speed of 3 mph. We believe that this speed, while accurate, could be improved with driver training or well programmed autonomy. The final attempt was over a second and a half faster than the initial attempt and the only change was that the student became more comfortable with the controls. More driver training would have improved the accuracy of the drive tests.

$$\text{Trial1} := 15.4\text{sec}$$

$$\text{Trial2} := 14.8\text{sec}$$

$$\text{Trial3} := 14.0\text{sec}$$

$$\text{Time1} := \frac{66\text{ft}}{\text{Trial1}} = 2.922\,\frac{\text{mi}}{\text{hr}}$$

$$\text{Time2} := \frac{66\text{ft}}{\text{Trial2}} = 3.041\,\frac{\text{mi}}{\text{hr}}$$

$$\text{Time3} := \frac{66\text{ft}}{\text{Trial3}} = 3.214\,\frac{\text{mi}}{\text{hr}}$$

$$\text{Average} := \frac{\text{Time3} + \text{Time2} + \text{Time1}}{3} = 3.059\,\frac{\text{mi}}{\text{hr}} \quad (10)$$

4.3 Thermodynamic Analysis

Because we kept the very top of the electronics box open with only a filter, we were able to use forced convection to cool the electronics. The CFM required given our current electronics setup was extremely low, so we were able to keep the electronics well below their maximum operating temperature and provide additional cooling to allow for potential electronic additions.

4.4 IP Goal

In accordance with our IP code testing plan, the AFIA robot was splashed with water from a variety of angles. The two key testing angles were 45° from the ground and straight down on the lid. The 45° angle had the most water coming in contact with the filter and beeswax cloth. This test was designed to ensure the cloth and filter were capable of keeping water out of the electronics box as the robot drove through water. One of the largest concerns was leakage of water through the t-nuts in the event of water falling directly onto the lid. The electronics box was filled with paper towels in order to better assess any failure points. In addition to structured testing, the robot was left outside for fifteen minutes during moderate rainfall. Once the robot was brought inside, we checked the paper towels to determine how much water entered the box. Even with the addition of rain, the paper towels were completely dry, as shown in Figure 34.

Figure 34: Water Ingress Testing and Results

The dust goal was tested using a small section of filter. Based on the water tests that showed the lid and beeswax fabric were completely sealed, we concluded that the filters to be the potential dust entrance. The filters used were rated to remove all large airborne particles and reduce the ingress of dust. This was verified by attempting to force dirt and sand through the filter. Only fine grains, less than 0.25 mm in size, were able to pass through, and then only with substantial force; otherwise, no particles passed through the filter. This test showed that while the filter was not dust-tight, it was sufficiently dust resistant. Based on these tests we determined that the AFIA robot met the primary IP goal.

4.5 Code Capabilities

The AFIA robot was able to be operated using an RC controller. The teleoperation control code was able to map the pulse from the controller onto motor values. These values were passed to the SPARK motor controllers as a PWM signal that controlled motor motion. The augmented autonomy was capable of reading and processing data from the ultrasonic and infrared sensors to detect ditches and obstacles. The infrared sensors were placed at the forward ends of the PVC legs at a -30° angle from horizontal. The placement and geometry of the infrared sensors is shown in Figure 35.

Figure 35: Infrared Range Finder Placement Angle

To ensure that our program was able to accurately detect the ditch size we checked it against flat ground and a known obstacle of 5.5 inches. The setup for the obstacle can be seen below in Figure 36. We found that the IR sensors readings fluctuated, without a change in ditch depth. To remedy this, we used running averages which was able to help us get a more accurate reading.

Figure 36: IR Test Set-Up

If an obstacle was detected that exceeded the set safe size, in this case 6 inches, the augmented autonomy successfully overrode the drive code and stopped robot functions. In order to reinstate driving functions, the driver had to pulse channel 3 on the RC controller.

4.6 Terrain Capabilities

We tested AFIA on different types of terrain around campus. We measured the curbs on campus and found them to be six inches tall. We used these curbs to test our primary terrain goal. AFIA was able to drive over and off of curbs without damage. From our test we found that the rocker was able to ensure that the robot maintained contact on the ground even while driving over large obstacles as seen in Figure 37.

Figure 37: Drivetrain Testing in a Ditch

Because of the torque produced by motors, even with the sinkage expected when driving in dirt and grass, AFIA was able to drive up steep inclines. The exception being when AFIA attempted to drive through mulch. Once three of the wheels sunk into the mulch, the robot lost traction and was unable to continue. This can be seen in Figure 38.

Figure 38: Drivetrain Testing in Loose Ground

Overall, given our testing, AFIA should be able to drive even on the worst roads in Ghana with little difficulty.

4.7 Battery Goal

Originally seven batteries were ordered for the AFIA robot which would allow for the full run time of two hours. Unfortunately, there was a delay in the order process and the batteries went out of stock. The AFIA team was able to acquire two batteries which allowed for thirty minutes of testing, and extrapolated expected results from a full run time with seven batteries from the data collected from the two battery test. Based on a full day of testing which involved driving the robot around campus on a variety of terrains and timing the battery life, two batteries provided a little over half an hour of drive time, specifically 35 minutes. This means that with seven batteries, the AFIA robot would run for 122 minutes. It is worth noting that towards the end of the test, the overall robot speed decreased to the point of stopping and, in the end, the students had to carry the robot back to the lab.

4.8 Growth Potential

In keeping with our goal of longevity and ability to be adapted to future useful applications as they arise, our testing plan included focus on two areas of growth potential: additional sensors and additional payload. As sensor capability is something we included attachment space for in the electronics design for our PCB, which ultimately could not be printed in time, this was something we could not formally test. For accessory payload capacity, we had a specific weight handling goal of up to 20lbs. To test this, we loaded the robot with four bricks in addition to those used to account for the missing batteries, each weighing about 5 pounds. Once these weights were set in place, we proceeded to drive the robot along a short track, to ensure it was still capable of normal operation with the extra payload.

4.9 Material Considerations

While we were unable to utilize exclusively tier 1 and tier 2 materials, we were able to drastically minimize the number of imported materials. The only frame materials that are not from tier 1 or 2 are metal components at critical points. While we attempted to make them out of sustainable, locally sourced materials, it was not feasible on account of the dynamic forces acting on the rocker. Even with some imported materials, robots like AFIA have the potential to expand accessibility of robotics to sub-Saharan countries.

4.10 Overall Design and Construction

While there were some last-minute changes to the battery drawer and rocker connections, the AFIA design proved that non-standard materials could create robust robotic systems. The design of the electronics box and rocker system were not only able to meet material and ingress protection goals but also, with a stronger connection, overcome the desired obstacles. It is flexible and able to be customized based on the desired operation. The best example of this is how additional space in the electronics box, allocated for the addition of sensors or payloads, became battery storage.

5. Conclusions

5.1 Recommended Improvements

5.1.1 Handling Loads at Pivot Points

There were a number of assembly components that did not perform as we had expected they would, starting with the t-nuts in our rocker. The t-nuts that made up our standard bolting pattern, set into the lid of the electronics box, were perfectly serviceable. However, those that experienced a significant load, where unable to support the required forces without popping out, ultimately causing the robot to fail. Instead of their teeth helping them keep a grip on the wood and stay in place, the motion of the robot continually pressed them outward. Even set in deeply, reinforced with super glue, and braced by an additional oak support the t-nuts strained to pop out, causing bowing of the legs and loss of rocker motion.

The original design called for ½-inch shoulder bolts. While in theory this seemed like it would work as they were a standard COTS part, it became clear upon assembly that they were not capable of holding the rocker. Because the shoulder bolts only connected on two points, the rocker bowed, causing uneven load distribution on the wheels, which ultimately made the robot unable to drive.

To remedy this, we decided to remove the battery drawer and replace it with an axle that went through the entirety of the robot. Before purchasing additional materials to implement this late-stage change, we tested this design with a hollow aluminum tube that was already in the lab. This test, while ultimately unsuccessful as the dynamic forces proved too great for the hollow tube, verified the load-bearing capability of the design. Results from this test can be seen below in Figure 39.

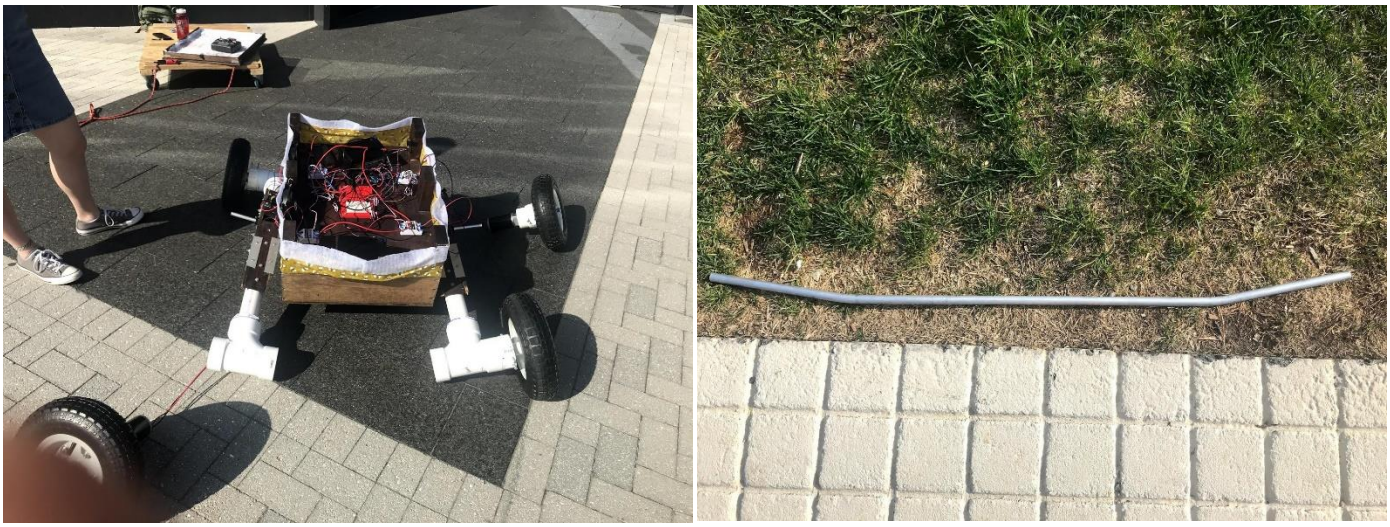

Figure 39: Hollow Aluminum Axle

With the design verified, we purchase a solid steel axle of the same size. The solid steel stock was able to better handle the dynamic load applied at that point but after brief testing, the wood cracked causing one side of the rocker to come off. It became clear that because of the dynamic forces acting on the pivot points that they must be reinforced by metal. We added ⅛-inch thick aluminum plates to either side of the rocker legs at the pivot point to ensure that they could withstand the forces to which they will be subjected. These reinforcing plates can be seen below in Figure 40.

Figure 40: Reinforcing Aluminum Plates

5.1.2 3D Printing

3D printing was unable to provide the structural support required for load bearing components. This, coupled with the high tolerance required for sizing, ultimately caused the 3D printed parts to crack. The external curve of the 3D printed gearbox holders caused the bolt holes to distort. Some were ovaloid rather than circular, and others had large PLA ridges inside. Both conditions prevented the bolts from going in easily and caused problems with aligning the bolts and the gearbox bolt holes. A more accurate print or a different fabrication method would have simplified motor installation by decreasing the amount of work required to accurately fit the bolts through the plastic holders.

5.1.3 Parts Acquisition

On a number of occasions construction was stalled due to lack of materials. Rather than having organized trips to the hardware store to buy everything we needed for that stage of building, we tended toward small runs to pick up single parts we found ourselves lacking. This caused delays as we waited for required materials and was something we could have remedied by planning out that aspect of our project more carefully. For construction of the battery drawer, we organized a cut list, purchased all the necessary lumber and additional supplies, and had the parts cut in a single session, resulting in having everything for that stage of construction ready to be assembled after one day's work. Applying that methodology to the rest of parts acquisition is a change that were we to do this project over again, we would be quick to make.

5.1.4 Design for Construction

Another area that could have been improved upon was in designing for construction. One of the primary goals of the AFIA MQP was for our robot to be built of low-cost materials readily available in sub-Saharan Africa. This means it is in large part made up of wood, rather than traditional engineering metals, and while we considered the difference in weight, strength, and stress properties, we did not always appreciate the ways constructing a robot of wood would differ from construction with metal. From details such as wood's tendency to split or splinter without pre-drilling, to more overarching issues such as the lack of woodworking facilities

available to us, construction from wood was not always as simple as we had expected. Ultimately a fair deal of our parts were cut using a jigsaw, and while that generous loan helped us work much more smoothly forward with our construction, a jigsaw is less smooth and precise to operate than a table or even circular saw would have been. Any number of times the simple question of 'how are we going to build this?' stalled us briefly, before replacing the more ideal answer of 'with a woodshop', something we did not have access to, with 'cutting very carefully with a jig- or hacksaw'. In the future, we would know to more carefully consider not only what materials to use, but also how to work with the materials we chose, in our design and construction plans.

An issue that was somewhat compounded by these difficulties working with wood in facilities meant more for metalwork was the extreme precision of many of our build components, especially those most critical. Their importance meant much careful planning and calculation went into planning exact shapes and dimensions, to ensure various components' strength, bending, support, and motion capabilities. But in practical building terms, having dimensions to the thousandths decimal place, not accounting for blade loss when tolerancing small and vital components, dimensioning holes that did not match up to any standard drill bit, and other such oversights made construction at times much more difficult than it needed to be. Overall, we would say that in the future, attention would have to be paid not only to the most optimal design, but how it will be built with consideration to the build materials themselves as well as the building facilities available for use.

5.1.5 PCB Design

One of the goals of the project was to create a PCB shield for the Arduino to simplify the wiring process. Because it was a secondary goal and was not required for basic testing, the deadline for the PCB shield got shifted back significantly. When the board did arrive, it was quickly discovered that the grounds were not properly connected in the design causing the board to be completely unusable. Because of the time crunch, the PCB design was fixed but was unable to be fabricated. By starting this process earlier, we could have gone through more iterations of the PCB and thus found and remedied issues pertaining to it earlier.

5.1.6 Testing Earlier

In the case of the AFIA project there was no way to have begun testing earlier without abandoning large and vital aspects of the design. We were faced with the usual construction delays as well as COVID-19 restrictions that limited lab access. This being said, if testing had begun earlier, then the presentation and reporting process would also have gone smoother and included more reflection and analysis.

5.2 Areas of Strength

5.2.1 Teamwork

Something that helped carry our team through various setbacks, frustrations, unexpected circumstances, and more was our team dynamic and ability to work together. While it was by no means always easy, we each stayed committed to treating each other with compassion and respect. This allowed us to extend understanding and support to one another when any of us was falling behind, comfortably work through differences of opinion, and motivate each other to push forward when the time came for hard work. Each of us had full confidence in the others' dedication and commitment and was eager to extend a hand to a teammate in need, keeping stress low, and productivity and morale high.

5.2.2 Parametric CAD

One of the crucial aspects of any successful MQP is being able to respond to required changes quickly. For us, part of that was needing to be able to quickly alter dimensions in our Solidworks model without breaking the entire assembly. We were able to utilize parametric features in Solidworks to enact more swift and efficient changes in the model with ease.

5.3 COVID-19 Considerations

The COVID-19 pandemic affected every aspect of life this year and the AFIA project was no exception. WPI had to close campus buildings twice during the academic year. During these closures, students were not allowed to participate in lab classes in person. For the first closure there were no separate instructions publicized for MQP lab work. The AFIA team erred on the side of caution and treated the project as a lab class. This led to a combined month of build time lost. The time we were able to spend in the lab was complicated by school policies that, for much of the winter, only allowed one team member to be working on the robot at a time. The remaining team members had to be six feet away and could not touch the equipment or assembly. Altogether these restrictions, valued and observed for the protection they offered our community, continually slowed and interrupted progress on the AFIA project in ways unseen in years previous.

5.4 Future Potential

There are multiple directions on which a future iteration of the AFIA MQP could choose to focus. Looking back at our mission scenario there are two main routes that we recommend future teams consider.

The first route would involve adding additional autonomous features to AFIA, so that it could traverse these remote roads without a human operator. This would involve being able to track AFIA through the run duration, decision making capabilities in relation to obstacles instead of just stopping, and sensors to autonomously ensure that the robot stays on the road.

5.5 Overall Conclusions

The overall aim of AFIA was to design and build a robot capable of handling rough terrain out of low-cost, sustainable materials widely available in sub-Saharan Africa to serve as a modular base platform for investigating accidents and expanding awareness and use of robotics in the region. Looking back, there are a number of changes to the design, parts used, and planning the team would have made. Most prominently, we would have involved more use of metals, primarily

steel and aluminum, at critical points. Though metal was a tier 3 material, it provided vital support in areas where the alone wood failed, such as the bracket arms. Given these failures, we believe that adding more metal to crucial parts of the rocker outweighs the downsides of increased use of tier 3 materials. With the metal supports, our robot was able to meet the majority of our goals and shows potential regarding its ability to traverse difficult roads in Ghana. While AFIA is a prototype, we believe it demonstrates the feasibility of non-standard materials for use in mobile robotic platforms, even in rough terrain.

References

1. “Drones to start delivering vaccines, blood across Ghana,” *New York Post,* 2019, https://nypost.com/2019/04/25/drones-to-start-delivering-vaccines-blood-across-ghana/.
2. “Zipline - Global public health,” Flyzipline. https://flyzipline.com/solutions/global-public-health/.
3. “Vaccines by air as drone medicine service takes off in Ghana,” *The Guardian,* 2019, https://www.theguardian.com/global-development/2019/apr/25/medical-delivery-drones-cleared-for-takeoff-in-ghana-zipline.
4. “Tapping Into Ingenuity,” *Brand South Africa,* 2008, https://www.brandsouthafrica.com/people-culture/people/tapping-into-ingenuity010708.
5. Gunawan, I. and Murphy, T., “How Playpumps are an example of learning from failure”. *Humanosphere,* 2013. http://www.humanosphere.org/basics/2013/07/how-playpumps-are-an-example-of-learning-from-failure/
6. P. F. Santana, J. Barata, and L. Correia, “Sustainable robots for humanitarian demining,” *International Journal of Advanced Robotic Systems*, vol. 4, no. 2, p. 23, 2007.
7. P. Santana, C. P. Santana, P. Santos, L. Almeida, L. Correia, and J. Barata, “The Ares Robot: Case study of an affordable service robot,” *Second European Robotics Symposium 2008,* Jan. 2088.
8. McLeod, B. K., Eccles, B. J., Wills, M. E., Watson, T. J., & Murcko, T. M. (2015). *WALRUS Rover MQP*. Retrieved from https://digitalcommons.wpi.edu/mqp-all/1747
9. Amato, J. L., Anderson, J. J., & Carlone, T. J. (2011). *ORYX 2.0 A Planetary Mobility Platform.* https://digitalcommons.wpi.edu/mqp-all/3570/
10. Pepicelli, C. M., Wolanin, C., Entov, G., Tai, J. L., Mao, L., & White, S. S. (2019). Kinisi: A Platform for Autonomizing Off-Road Vehicles. Retrieved from https://digitalcommons.wpi.edu/mqp-all/7093
11. “The IP Code: A guide to waterproof and dustproof ratings,” Reactual. https://reactual.com/portable-electronics/understanding-ip-code.html#:~:text=The%20solid%20particle%20protection%20is,is%20completely%20dustproof%20and%20waterproof.

12. “Thermal radiation,” Encyclopedia Britannica. https://www.britannica.com/science/thermal-radiation.
13. P. Múčka, “International Roughness Index specifications around the world,” *Road Materials and Pavement Design*, vol. 18, no. 4, pp. 929–965, 2016.
14. “The best time to travel to Ghana.” USA Today. https://traveltips.usatoday.com/time-travel-ghana-18251.html
15. “Average weather in Accra, Ghana year round.” Weather Spark. https://weatherspark.com/y/42322/Average-Weather-in-Accra-Ghana-Year-Round.
16. “Roughness,” Pavement Interactive. https://pavementinteractive.org/reference-desk/pavement-management/pavement-evaluation/roughness/. [Accessed: 12-Sep-2020].
17. “Ackermann steering geometry,” *Wikipedia*, 29-Apr-2021. [Online]. Available: https://en.wikipedia.org/wiki/Ackermann_steering_geometry. [Accessed: 04-May-2021].
18. M. Cullen, S. Diamond, W. Dunn, and K. Gimsley, “Optimal Driveline Robot Base,” May 2014.

19. “Continuous track,” *Wikipedia*, 08-Apr-2021. [Online]. Available: https://en.wikipedia.org/wiki/Continuous_track. [Accessed: 04-May-2021].
20. “Wheels,” NASA, 20-Aug-2019. [Online]. Available: https://mars.nasa.gov/msl/spacecraft/rover/wheels/. [Accessed: 26-Oct-2020].
21. “What are the reasons behind using rocker bogie suspensions in mars curiosity rover?,” *Quora*. [Online]. Available: https://www.quora.com/What-are-the-reasons-behind-using-rocker-bogie-suspensions-in-mars-curiosity-rover. [Accessed: 04-May-2021].
22. F. Castellani, “THE SCIENCE OF SOLVENT WELDING A technical presentation for specifiers and owners about the inner workings of solvent cements,” *Weld On*. [Online]. Available: https://weldon.com/wp-content/uploads/2015/03/Weld-On_The_Science_of_Solvent_Welding.pdf. [Accessed: 07-Apr-2021].
23. “12V 100Ah AGM Sealed Lead Acid Battery,” *amazon.com.* [Online]. Available: https://www.amazon.com/100Ah-Sealed-Battery-UB121000-Group/dp/B00BMUDOLE. [Accessed: 6-Nov-2020].

24. “WindyNation 100Ah 12V AGM Deep Cycle Sealed Lead Acid Battery,” *amazon.com.* [Online]. Available: https://www.amazon.com/WindyNation-amp-Hour-100AH-Sealed-Battery/dp/B07BS1ZB15. [Accessed: 7-Nov-2020].
25. “12V 100Ah Rechargeable Sealed Lead Acid Battery,” *homedepot.com.* [Online]. Available: https://www.homedepot.com/p/MIGHTY-MAX-BATTERY-12-Volt-100-Ah-Rechargeable-Sealed-Lead-Acid-SLA-Battery-ML100-12/308914703#product-overview. [Accessed: 7-Nov-2020].
26. “12V 100Ah Lithium Ion Battery,” *lithiumion-batteries.com.* [Online]. Available: https://www.lithiumion-batteries.com/products/product/12v-100ah-lithium-ion-battery.php. [Accessed: 8-Nov-2020].
27. “GreenLiFE Battery GL100 - 100Ah 12V Lithium Ion Battery,” *amazon.com.* [Online]. Available: https://www.amazon.com/GreenLiFE-Battery-GL100-100AH-Lithium/dp/B01NAV9G9X. [Accessed: 9-Nov-2020].
28. “100Ah Lithium Battery,” *amazon.com.* [Online]. Available: https://www.amazon.com/100ah-lithium-battery/s?k=100ah+lithium+battery. [Accessed: 9-Nov-2020].
29. “12V 16Ah Deep Cycle LiFePO4 Battery,” *amazon.com*. [Online]. Available: https://www.amazon.com/gp/product/B07X7MD2JK/ref=ppx_yo_dt_b_asin_title_o00_s00?ie=UTF8&psc=1. [Accessed: 10-Nov-2020].
30. “12 Volt 3.2 Ah Sealed Lead Acid Rechargeable Battery,” *batterymart.com*. [Online]. Available: https://www.batterymart.com/p-12v-3_4ah-sealed-lead-acid-battery.html. [Accessed: 6-Nov-2020].
31. “12 Volt 22 Ah Sealed Lead Acid Rechargeable Battery,” *batterymart.com.* Available: https://www.batterymart.com/p-sla-12v22.html. [Accessed: 9-Nov-2020].
32. “SPARK Motor Controller,” *REV Robotics*. [Online]. Available: https://www.revrobotics.com/rev-11-1200/. [Accessed: 31-Oct-2020].
33. “Cooling Flow Calculation,” *AMETEK ROTRON*. [Online]. Available: https://www.rotron.com/tech-corn/cooling-flow-. [Accessed: 11-April-2021].
34. “LV-MaxSonar-EZ Series,” *maxbotix*. [Online]. Available: https://www.maxbotix.com/documents/LV-MaxSonar-EZ_Datasheet.pdf. [Accessed: 25-Oct-2021].

35. “Pololu - Sharp GP2Y0A21YK0F Analog Distance Sensor 10-80cm,” *Pololu Robotics & Electronics*. [Online]. Available: https://www.pololu.com/product/136. [Accessed: 25-Oct-2020].

Appendices

Appendix A: Pictures of Ghanaian Roads

Figure 41: Roads in and Around Akyem Dwenase, Eastern Region, Ghana

Appendix B: Key Project Dates

Deadline:	Date:
Desired Travel Speed Selected	9/30/2020
Final Proposal Submitted	10/4/2020
Import Cost Research Completed	10/8/2020
Materials Research Completed	10/8/2020
Chassis Simulink Simulation Completed	10/16/2020
Initial Chassis CAD Completed	10/26/2020
Sensor Selection Completed	11/2/2020
Breadboard Prototype Completed	11/8/2020
Box Material Research Completed	11/9/2020
Initial Box CAD Completed	11/13/2020
Cooling System Design Completed	11/18/2020
Box and Cooling Prototype Completed	11/24/2020
Code Outline Completed	11/24/2020
PDR Date	12/4/2020
Methodology Draft Completed	1/4/2021
Box Construction Complete	1/31/2021
Teleoperation Code Complete	2/5/2021

Board Design Completed	3/21/2021
Chassis Construction Complete	4/10/2021
Sensor and Board Testing Complete	4/23/2021
System Integration	4/23/2021
Local System Testing	4/23/2021
New Sensor Integration	4/23/2021
Presentation Poster Due	4/26/2021
Box and Cooling Software Testing	4/28/2021
Chassis Testing	4/28/2021
Project Presentation Day	4/30/2021
Payload Capacity Testing	5/3/2021
Final System Test	5/3/2021
Final Report Due	5/6/2021

Table 10: Key Project Dates

Appendix C: Budget Estimate

Item	Price per part	# of Parts	Total Cost	Notes
DriveTrain				
Rope for tension	$5.00	1	$5.00	Buy by 50 ft coil for paracord (priced according)
PVC	$4.00	4	$16.00	sold by 10 ft.
Wood	$15.00	4	$60.00	for 2'x2' sheet of 1/2" ply
Motors	$50.00	4	$200.00	
Bolts	$20.00	1	$20.00	All the bolts needed for the entire project
Pipe Clamps	$3.00	15	$45.00	prices vary from $0.10 to $30
Gears	$25.00	10	$250.00	
Axle (machined on Lathe)	$1.71	3	$5.13	Really cheap metal price per ft (budget for. 0.5" Diameter)
Wheels	$30.00	4	$120.00	
Prototyping Budget	$75.00	1	$75.00	
		Total Cost:	$796.13	
Electrical Box				
External Material	$0.00	0	$0.00	(Can use one of the prototyped boxs)
Prototyping Budget	-	-	$177.60	Makes 4 diffrent 1' prototypes
		Total Cost:	$177.60	
Electronics				
Batteries	$200.00	1	$200.00	
Microcontroller	$12.00	1	$12.00	Looking into Arduino Mega from Odoo or similar board
Custom Shield	$5.00	8	$40.00	per sq inch
Object Detection Sensors	$30.00	1	$30.00	
Inspection Display	$20.00	1	$20.00	
Motor Controller	$70.00	4	$280.00	
Prototyping Budget	$50.00	1	$50.00	
		Total Cost:	$632.00	

Total Cost of MQP:	$1,605.73
Dept money- Total Cost of MQP	-$855.73
Indivitual Contribution per person	$285.24

Table 11: Overall Budget

Possible Electronic box Prototypes (To make a 1' Cube)				
Item	Price Per Part	Number of Parts	Total Cost	Notes
Scrap Metal Box				
Metal	$35.00	1	$35.00	
Water Proofing Gusset	$9.00	4	$36.00	
			$71.00	
Rain Coat Box with PVC				
PVC	$0.40	12	$4.80	Calculated by Foot (Multiple Designs use PVC)
PVC Brackets	$4.00	6	$24.00	
Rain Coat	$10.00	1	$10.00	
Zipper	$3.00	1	$3.00	
		Total Cost:	$41.80	
Bees Wax Cloth Box with PVC				
PVC	$0.40	12	$4.80	Calculated by Foot (Multiple Designs use PVC)
PVC Brackets	$4.00	6	$24.00	
Fabric	$6.00	2	$12.00	
Bees Wax	$6.00	1	$6.00	
Zipper	$3.00	1	$3.00	
		Total Cost:	$49.80	
Storage Bin				Due to the nature of the storage bin, We can not make it just 1x1
Storage Bin with Lid	$15.00	1	$15.00	
		Total Cost	$15.00	

Table 12: Electronics Box Prototype Budget

Appendix D: Full PVC Stress Calculation

$W := -150lbf$ Weight of robot

$T2 := 135deg$ Angle between rocker legs

$L := 15.5in$ Length of rocker leg

$Od := 2.375in$ Outer diameter of PVC

$Id := 2in$ Inner diameter of PVC

$S := 7450psi$ Strength of PVC

$WpL := \frac{W}{2} = -75lbf$ Weight per rocker leg, assuming 2 leg conditions

$Fx := WpL \cdot \sin\left(\frac{T2}{2}\right) = -69.291lbf$

$Fy := WpL \cdot \cos\left(\frac{T2}{2}\right) = -28.701lbf$

Forces acting on one leg, assuming half box weight

$Ao := \left[\frac{Od}{2} \cdot (3.14)\right]^2 = 13.904in^2$

$Ai := \left[\frac{Id}{2} \cdot (3.14)\right]^2 = 9.86in^2$

$At := Ao - Ai = 4.044in^2$ Cross sectional area of PVC tube

$\frac{Fy}{At} = -7.097psi$ Force per area applied to PVC rocker leg

Appendix E: Full Motor and Gear Ratio Calculation

CIM Motor Calc

$w := 150lbf \quad v := 5mph \quad i := 15deg$ Variables, w = Weight, v = Velocity, i = Indine

$E := 0.03$

$P := w \cdot v \cdot \sin(i)$ Watts required to drive up incline

$P = 386.003\,W$

$P := 386W$

$\frac{P}{4} = 96.5\,W$ Watts per motor, currently 4 motors

$P1 := \frac{P}{(.97)^3} = 422.934\,W$ Power accounting for a loss of 3% per stage due to planetary gearbox

$P1 := 423W$

$\frac{P1}{4} = 105.75\,W$ Watts per motor, assuming 4 motors

Cim watts = 337

$MT := 4.4in \cdot lbf \qquad r := 6.5in \qquad Th := 45deg$

$T := w \cdot r \cdot \sin(Th) = 689.429 \cdot in \cdot lbf$ Torque necessary to climb 30 deg grade

$T1 := \frac{T}{.97^3} = 755.396 \cdot in \cdot lbf$ Torque accounting for a loss of 3% per stage due to planetary gears

$T1 := 755in \cdot lbf$

$T2 := \frac{T1}{4} = 188.75 \cdot in \cdot lbf$ Torque per motor

$\frac{T2}{MT} = 42.898$ Gear Ratio, rounded to 48

$GR := 48$

Appendix F: Motor Curve Data

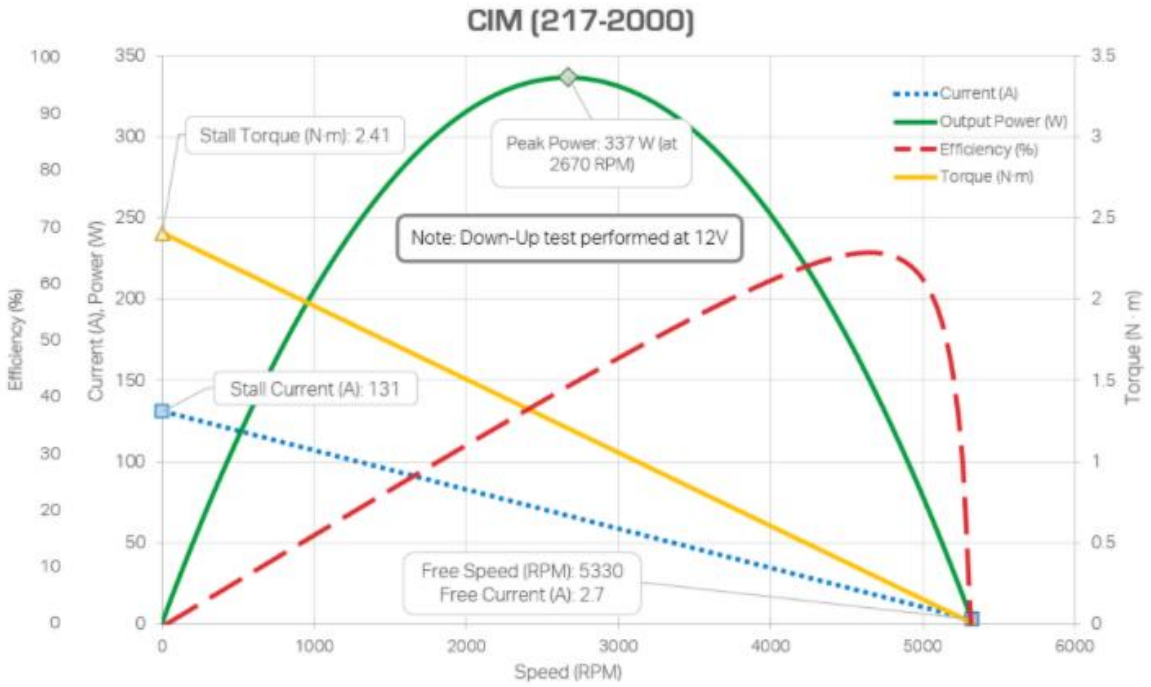

Figure 42: CIM Motor Curve

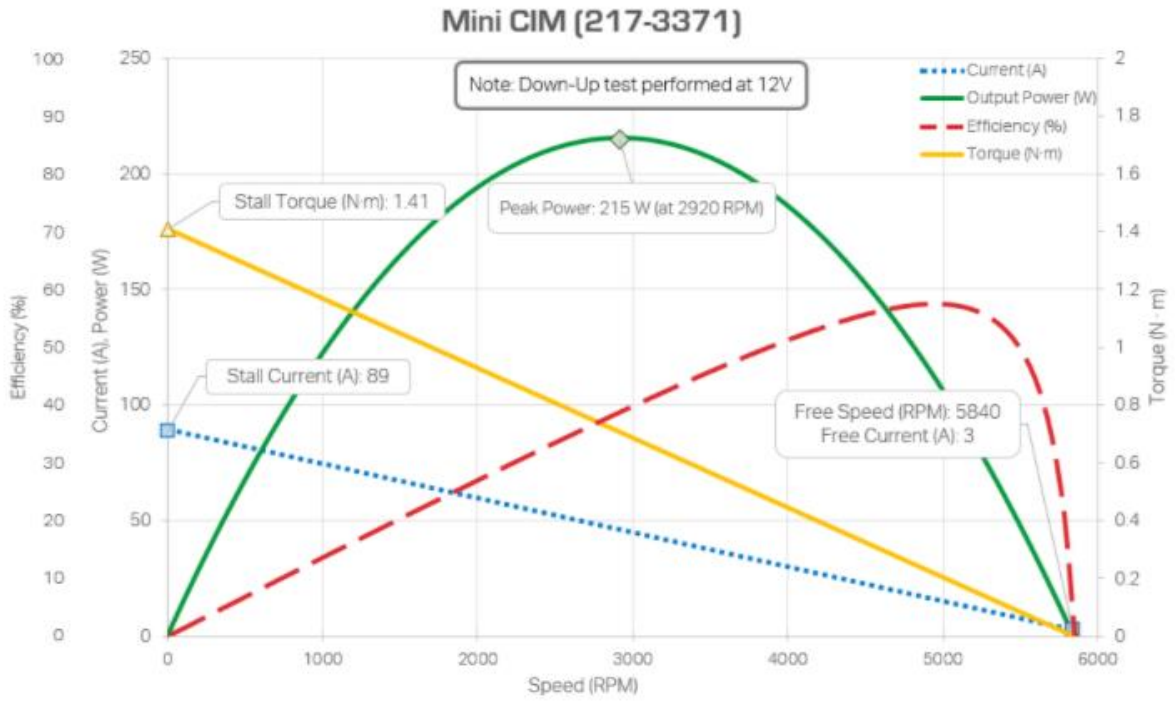

Figure 43: Mini-CIM Motor Curve

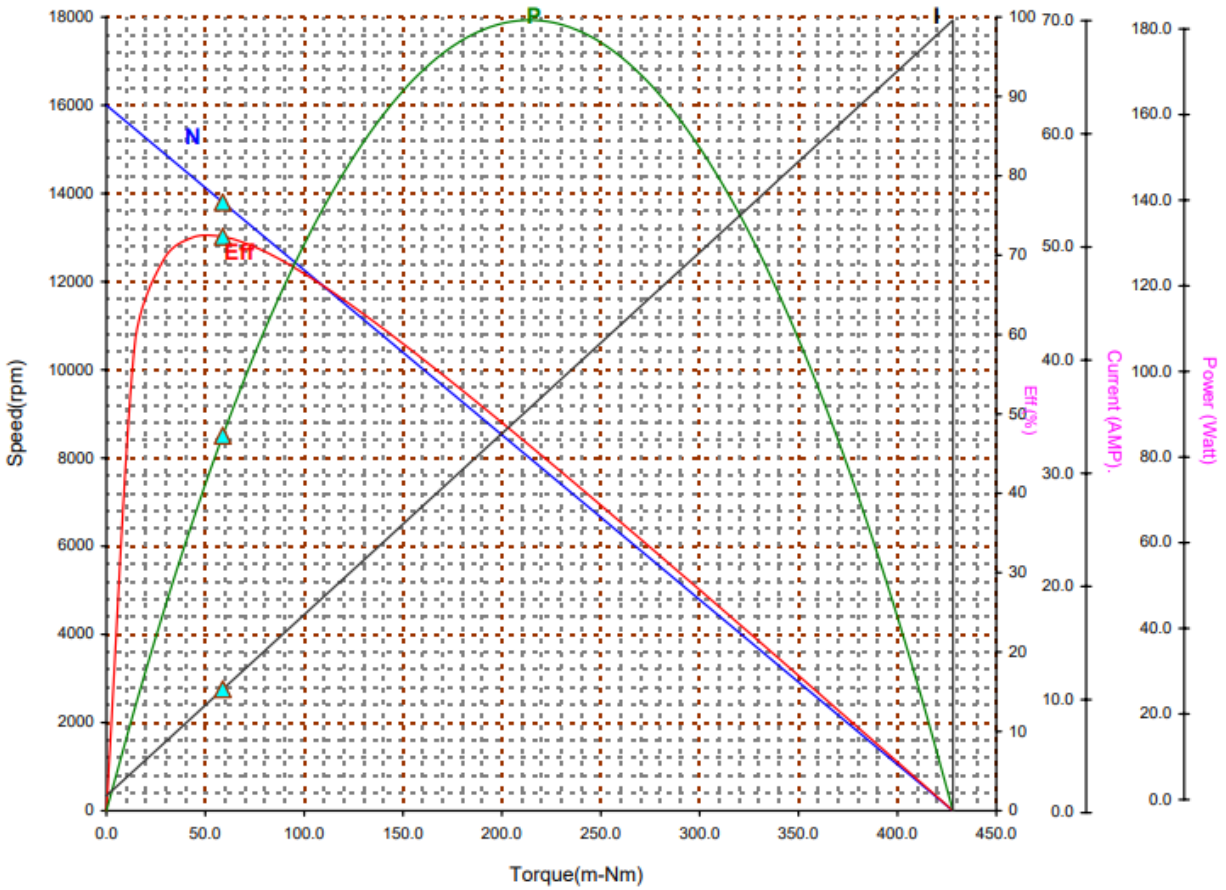

Figure 44: CCL 9015 Motor Curve

Appendix G: Full Battery Calculation

Lithium Iron Battery

$v := 12V$	$a := 16A$	$aH := 16A \cdot hr$	$C := 54$	$w := 3.97lbf$
voltage	current	amp hours		weight per battery

Operating on flat ground

$c := 12.8A$	necessary current for operation for one motor
$cT := c \cdot 4 = 51.2\,A$	for four motors
$aHT := cT \cdot 2hr = 102.4 \cdot A \cdot hr$	current for two hours
$b := \frac{aHT}{aH} = 6.4$	rounded to 7 batteries
$CT := C \cdot 7 = 378$	cost for 7 batteries
$wT := w \cdot 7 = 27.79 \cdot lbf$	weight of 7 batteries

Appendix H: GrabCAD Link (With CAD)

https://workbench.grabcad.com/workbench/projects/gc_YS72n6F7JJDQDdDTAdC-oNmu3EjQ301-Bh2C_VVaPTC#/space/gc9tG-CF76gNP670obWP9BnHbhHamUmpGeJ3YStFmmwfwq

Appendix I: Github Link for AFIA Code

Github.com/AFIAMQP